Few generalizable patterns of tree-level mortality during extreme drought and concurrent bark beetle outbreaks

Charlotte C. Reed *, Sharon M. Hood

USDA Forest Service, Rocky Mountain Research Station, Fire Sciences Laboratory, 5775 US Highway 10 W, Missoula, MT 59808, USA

HIGHLIGHTS

- Recent drought and bark beetles caused extensive tree mortality in California, USA.
- A three-proxy approach is used to elucidate risk factors for tree-level mortality.
- Living and dead trees exhibit some differences in growth, isotopes (Δ^{13}C) and defenses.
- Differences between living and dead trees are not consistent across species.
- Effects of drought with beetles mask generalizable risk factors of mortality.

GRAPHICAL ABSTRACT

Identified within-species risk factors for tree-level mortality due to the combination of severe drought and concurrent bark beetle outbreaks associated with the 2012–2016 California, USA drought. Risk factors are categorized by species and category of metric measured. While we do not attempt to disentangle the effects of drought and bark beetles, host-specific beetles were identified as contributing to mortality for ponderosa pine, pinyon pine, and white fir, while incense cedar showed no clear evidence of bark beetle attacks. BAI refers to basal area increment (i.e. radial tree growth), Δ^{13}C refers to discrimination of the heavier (^{13}C) carbon isotope measured from tree rings, and PDSI refers to the Palmer Drought Severity Index.
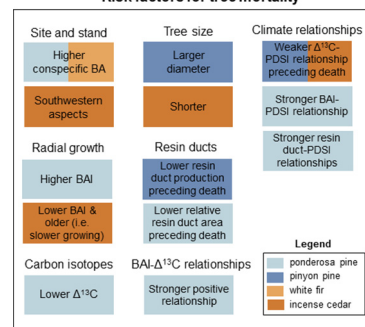
ARTICLE INFO

ABSTRACT

Tree mortality associated with drought and concurrent bark beetle outbreaks is expected to increase with further climate change. When these two types of disturbance occur in concert it complicates our ability to accurately predict future forest mortality. The recent extreme California USA drought and bark beetle outbreaks resulted in extensive tree mortality and provides a unique opportunity to examine questions of why some trees die while others survive these co-occurring disturbances. We use plot-level data combined with a three-proxy tree-level approach using radial growth, carbon isotopes, and resin duct metrics to evaluate 1) whether variability in stand structure, tree growth or size, carbon isotope discrimination, or defenses precede mortality, 2) how relationships between these proxies differ for surviving and now-dead trees, and 3) whether generalizable risk factors for tree mortality exist across pinyon pine (*Pinus monophylla*), ponderosa pine (*P. ponderosa*), white fir (*Abies concolor*), and incense cedar (*Calocedrus decurrens*) affected by the combination of drought and beetle outbreaks. We find that risk factors associated with mortality differ between species, and that few generalizable patterns exist when bark beetle outbreaks occur in concert with a particularly long, hot drought. We see evidence that both long-term differences in physiology and shorter-term beetle-related selection and variability in defenses influence mortality susceptibility for ponderosa pine, whereas beetle dynamics may play a more prominent role in mortality patterns for white fir and pinyon pine. In contrast, incense cedar mortality appears to be attributable to long-term effects of growth suppression. Risk factors that predispose some trees to drought and beetle-related

* Corresponding author.
  E-mail address: charlotte.reed@usda.gov (C.C. Reed).

mortality likely reflect species-specific strategies for dealing with these particular disturbance types. The combined influence of beetles and drought necessitates the consideration of multiple, species-specific risk factors to more accurately model forest mortality in the face of similar extreme events more likely under future climates.

Published by Elsevier B.V.

1. Introduction

Droughts have been linked to an increase in forest mortality events (Allen et al., 2010), with further drought-related impacts on forests predicted with continuing climate change (IPCC, 2014; Allen et al., 2015). Longer duration, higher frequency, and/or hotter droughts are expected to alter forests globally via changes in primary production (Zhao and Running, 2010), species composition (Lloret et al., 2009; Martínez-Vilalta and Lloret, 2016), species dominance (Cavin et al., 2013), and interactions with other disturbances (Dale et al., 2001). Often, biotic agents interact with drought to further exacerbate these changes by amplifying mortality (Anderegg et al., 2015). Bark beetles (Coleoptera: Curculionidae, Scolytinae) are one example of a biotic agent that interacts with drought, and are expected to experience changes in population dynamics and range expansion due to increasing temperatures associated with further climate change, leading to increased tree mortality particularly during extended drought periods (Bentz et al., 2010; Kolb et al., 2016).

The combined impacts of drought and insect outbreaks on tree mortality have important implications for predicting forest dynamics under climate change, yet forecasting tree mortality is one of the most uncertain processes in dynamic vegetation models (Bugmann et al., 2019). To more accurately predict ways in which global change will alter forest dynamics, models must be informed by a better understanding of how tree-level factors influence mortality probability when multiple disturbance agents co-occur (Anderegg et al., 2015). Some tree-level early warning signals for drought-related mortality have been identified, but few patterns have emerged across species, and most studies do not consider drought interactions with insects (Camarero et al., 2015; Cailleret et al., 2017; Cailleret et al., 2019; Liu et al., 2019). Similarly, despite recent advances in the understanding of physiological mechanisms underlying drought-related tree mortality (Sevanto et al., 2014; Adams et al., 2017), much remains unclear. This is especially true when insects are involved (Anderegg et al., 2015; Hartmann et al., 2018), as they can affect both tree carbon and water balance, important links to drought-related mortality (McDowell et al., 2008). A handful of studies have examined why some trees die and others survive in the face of drought combined with insect outbreaks (McDowell et al., 2010; Meddens et al., 2015; Csank et al., 2016), but there remains a lack of understanding of whether generalizable tree-level mortality risk factors or early warning signals exist across species in the face of these interacting disturbances.

The 2012–2016 extreme drought in California, USA provides a valuable opportunity to better understand mortality dynamics associated with a particularly hot, multi-year drought (Diffenbaugh et al., 2015) and concurrent bark beetle outbreaks affecting multiple tree species. The record-breaking drought and associated outbreaks killed an estimated 147 million trees, with the peak of mortality occurring in 2015–16 and forests in central and southern California being most impacted (Goulden and Bales, 2019; USDA Forest Service, 2019). As bark beetles are better able to overcome tree defenses during drought, both the magnitude and length of the drought enabled multiple species of bark beetles to reach outbreak levels, amplifying mortality for several, co-occurring tree species (Fettig et al., 2019). This type of extreme disturbance is expected to become more common under future climates (Allen et al., 2015; Kolb et al., 2016), making it important to understand to more accurately model future forest mortality.

Tree ring analyses are a valuable way to quantify multiple factors that affect susceptibility to drought-related mortality over climate change-relevant timeframes. Quantification of radial stem growth is common in studies that compare trees that die and those that survive drought (Cailleret et al., 2017). Radial growth is a useful metric for assessing changes in tree-level carbon balance, as it is generally a lesser priority for carbon investment than, for example, foliage and root development (Dobbertin, 2005). Lower radial growth has been shown to precede drought-related mortality in most instances (Cailleret et al., 2017), but not necessarily when bark beetle outbreaks co-occur (de la Mata et al., 2017; Cooper et al., 2018). Relationships between radial growth and climate seem to additionally vary between trees that die and those that survive drought with or without concurrent beetle outbreaks, with generally greater sensitivity of growth to a variety of climate variables for trees that die (Suarez et al., 2004; McDowell et al., 2010; Hereş et al., 2012; Csank et al., 2016).

When examined in concert with radial growth, stable isotope ratios in tree rings can further elucidate population-level differences in tree physiological vulnerability to drought and beetle-related mortality (McDowell et al., 2010), as isotopes can serve as a whole-tree, annually-resolved index of gas exchange (Farquhar et al., 1989; McCarroll and Loader, 2004). Stable carbon isotope ratios ($\delta^{13}C$) relate to the ratio of intercellular (c_i) to ambient (c_a) CO_2 concentrations, and are thus related to both stomatal conductance and photosynthetic demand (see 'Materials and methods' for further explanation). A few tree ring studies have used a two-pronged approach utilizing stable isotope analysis in concert with growth analyses to examine differences in carbon isotope ratios between surviving and dying trees in the face of drought (Hereş et al., 2014; Gessler et al., 2018) or drought combined with beetle outbreaks (McDowell et al., 2010; Csank et al., 2016), but have found inconsistencies across species and sites.

When drought occurs in combination with bark beetle outbreaks, intraspecific differences in tree defenses against beetle attack may influence mortality probability (Gaylord et al., 2013; Huang et al., 2020). Resin duct characteristics in the secondary xylem of *Pinus* spp. relate to resin flow and thus serve as a useful indicator of tree defense against bark beetles (Hood and Sala, 2015). Previous studies have found differences in various tree-ring derived resin duct metrics for trees that die versus those that survive beetle outbreaks, with greater investment in defenses for trees that survive (Kane and Kolb, 2010; Gaylord et al., 2013; Hood et al., 2015; Zhao and Erbilgin, 2019), sometimes at the apparent cost of lower growth (Ferrenberg et al., 2014; Kichas et al., 2020). However, bark beetle outbreaks of previous studies that examine resin ducts have not been associated with extreme drought periods as long and hot as the 2012–2016 California drought.

We use plot-level data combined with a three-proxy tree-level approach using radial growth, carbon isotopes, and resin duct metrics to evaluate 1) whether variability in stand structure, tree growth or size, carbon isotope discrimination, or defenses precede mortality, 2) how relationships between these proxies and climate differ for surviving and now-dead trees, and 3) whether generalizable risk factors for tree mortality exist across four species affected by the combination of drought and bark beetle outbreaks. We expected the likelihood of mortality to be higher for trees in stands with higher density of the same species due to the influence of host availability and competition on both beetles and drought-susceptibility of trees. We anticipated that trees that died would have lower radial growth, but not necessarily if the effects of beetles overshadowed those of the drought (Cailleret et al., 2017), and be more sensitive to climatic stress (McDowell et al., 2010). Similarly, we expected carbon isotope discrimination to be lower, indicating chronic water stress (Warren et al., 2001), and for

trees that died to have fewer resin duct defenses (Kane and Kolb, 2010). To our knowledge no study has investigated drought impacts using this three-proxy approach for multiple species to shed light on how forests respond to extreme drought and bark beetle outbreaks that are increasingly likely to occur under future climate conditions.

2. Materials and methods

2.1. Study species and site selection

Sampling areas were established in two separate geographical areas affected by the 2012–2016 California drought and concurrent beetle outbreaks. Plots were established in southern California on the Los Padres National Forest (LP) to assess singleleaf pinyon pine (*Pinus monophylla* Torr. & Frém) mortality, and in central California on the Sierra National Forest (SNF) to assess ponderosa pine (*Pinus ponderosa* Lawson & C. Lawson), white fir (*Abies concolor* (Gord. & Glend.) Lindl. Ex Hildebr.), and incense cedar (*Calocedrus decurrens* (Torr.) Florin) mortality (Fig. 1). Pinyon pine occurs at relatively low elevations in comparison to other conifers in the region, growing close to its physiological limits near the southwestern extent of its range (Cole et al., 2008) and is a primary host to pinyon ips (*Ips confuses* LeConte). Soils in the LP area are primarily mollisols and are well-drained (NRCS, 2019). Ponderosa pine, white fir and incense cedar co-occur on the western slopes of the southern Sierra Nevada at mid-low elevations and serve as primary hosts to western pine beetle (*Dendroctonus brevicomis* LeConte), fir engraver beetle (*Scolytus ventralis* LeConte), and cedar bark beetles (*Phloeosinus spp.*), respectively. Soils in the SNF area are primarily inceptisols, with some occurrence of entisols at higher elevations and alfisols at lower elevations, and are well to excessively drained (NRCS, 2019).

Plots in the SNF sampling area utilized an extensive existing network where plots were initially installed on a randomly placed grid within areas of specific forest type, mortality level, and excluding areas of recent forest management (Pile et al., 2019). A subset of fifty plots in the network were selected for sampling in 2016 based on mortality level determined from 2015 Aerial Detection Survey (ADS) data and species composition. In order to capture a range of mortality levels across stands, approximately half of the plots were selected based on low mortality (<5%), and the other half based on relatively high mortality (>40%). Plots were primarily concentrated below 2134 m as drought effects were less pronounced at higher elevations. Plots in the LP sampling area were selected based on pinyon pine presence and mortality levels similarly determined from ADS data. Individual plot selection was random within areas of high and low mortality with pinyon pine dominance. Plots in both areas were required to have greater than 10.3 m^2 basal area and tended to be grouped in distinct clusters across the study areas due to the initial targeting of areas of high and low mortality. Distance between plots ranged from approximately 50–320 m while distances between distinct plot cluster centers ranged from 1 to 7 km.

2.2. Field measurements

We installed fixed area 0.04 ha circular plots in 2016 and assessed tree status annually through 2019 to monitor changes in mortality. Twenty-seven plots were installed in the LP sampling area, and 49 in the SNF area. One plot in the SNF area burned in 2017 and therefore was excluded from analyses. Plot-level measurements included elevation, slope, and aspect. For mortality monitoring, all trees >12.7 cm in diameter at breast height (DBH; 1.37 m) were tagged and measured for diameter and height during plot establishment. DBH was used as the measure of diameter for all species except pinyon pine. Diameter is more appropriately assessed at root collar (DRC) for these low-statured, forked trees. We recorded tree status (live or dead) and beetle attack status (unattacked, current successful attack, prior successful attack) for all trees. Mortality agent was assessed for dead trees based on

presence and pattern of insect-specific galleries (Wood, 1982) in order to determine the degree of mortality for each tree species attributable to host-specific bark beetles. We additionally calculated the proportion of trees of each species for which mortality was attributable to the drought and/or bark beetles. Trees that died during the drought and beetle outbreak are henceforth referred to as either dead or dying trees. It was impossible to discern if mortality was due to either drought or mass attack by a primary bark beetle species, as nearly all dead trees, with the exception of incense cedar, had evidence of beetle attack (western pine beetle for ponderosa pine, pinyon ips for pinyon pine, and fir engraver for white fir) and all trees experienced the drought. We collected tree-level data for all species within a plot, but subsequent analysis was limited to the best-represented species (i.e. pinyon pine, ponderosa pine, white fir, incense cedar). We later calculated measurements of stand density (e.g. trees per hectare, basal area) based on tree information at the plot level for use in mortality models.

2.3. Tree-ring sampling and processing

In 2016 at each plot we collected two, 4.5 mm-wide increment cores at DBH/DRC from two live and two dead trees of each species present (> 12.7 cm DBH/DRC), if available. While we did not target trees with specific canopy positions, trees with a clearly suppressed canopy position were largely excluded (< 4% of all cored trees). High mortality resulted in a number of plots having only dead trees to core and a few of the live trees cored in 2016 subsequently died between 2016 and 2018. These cores were moved to the dead category for analyses. As drought and beetle-related mortality typically occurs over several years, it is important to include trees that died over the course of this mortality event, but which may not have died immediately, in analyses. A lack of dead incense cedar and live ponderosa pine necessitated coring of additional trees within plots in 2017 and 2018 for more robust species-specific chronology development. For growth analyses and species-specific chronology building, we prepared cores using standard techniques (mounted and sanded until cellular structure was visible through a binocular microscope) and scanned whole cores using an Epson platform scanner at 1200 dpi. We assigned the calendar year to each tree ring (i.e. crossdated; Stokes and Smiley, 1968, Schweingruber, 1996, Cook and Kairiukstis, 2013) and measured ring widths to the nearest 0.001 mm using CooRecorder v7.8 (Cybis Elekronik & Data AB, Saltsjöbaden, Sweden). Crossdating was checked with COFECHA (Holmes, 1983). Series intercorrelations of chronologies ranged from a low of 0.48 for incense cedar to a high of 0.72 for pinyon pine (Table S1). We used 2018 data for all tree-level analyses as this was the final year of tree core collection, and mortality levels did not change much between 2018 and 2019 (53% and 54%, respectively). We originally cored 84 pinyon pine in the LP area and 69 ponderosa pine, 89 white fir and 93 incense cedar in the SNF area. Cores that could not be confidently crossdated or for which a pith distance could not be reasonably estimated (LP = 23%; SNF = 45% of cores) were eliminated from further analyses. For assessment of radial growth, ring widths were converted to basal area increment (BAI), which accounts for decreasing ring widths with increasing tree size (Biondi and Qeadan, 2008). Annual BAI values were calculated for each core and averaged by tree using the 'dplR' package in R (Bunn, 2008). Mean chronology length ranged from 118 (±4.2; S.E.) years for pinyon pine to 78 (±1.9) years for white fir, but chronologies were truncated to 1949-present for all trees, as this limited chronologies to years with sample sizes of at least 10 and years for which climate data consistently exist.

We randomly selected a subset of 6 live and 6 dead trees per species from the pool of datable cores for stable carbon isotope analysis, as is recommended by Leavitt (2010), with the requirement of tree dominance or co-dominance within the canopy. Because we selected these trees for similarity in canopy position, differences in diameter and height between live and dead individuals were not significant ($p > 0.1$). Cores used for
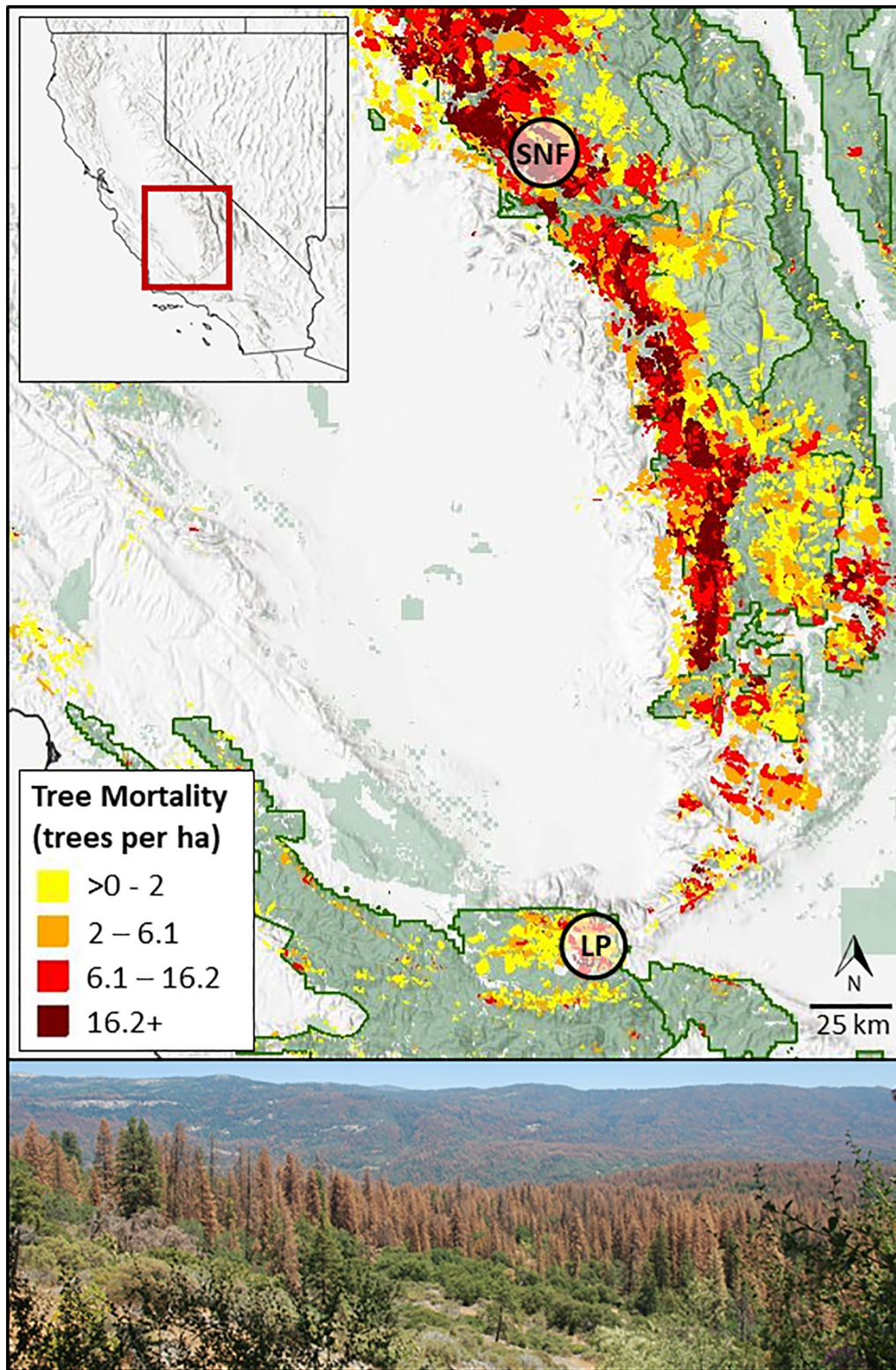
Fig. 1. Circles indicate general locations of study plots on the Los Padres National Forest (LP) and Sierra National Forest (SNF) overlaid on density of dead trees (trees per ha) due to the 2012–2016 drought and bark beetle outbreaks. Image of tree mortality extent on the SNF (below). Tree mortality determined from 2012 to 2016 Arial Detection Surveys (ADS) with data available: https://egis.fire.ca.gov/TreeMortalityViewer/.

isotope analysis were planed using a core microtome (Gärtner and Nievergelt, 2010), crossdated to determine year of ring development, and cut apart with a scalpel at each ring boundary for years 1956-present. The 1956 cutoff ensured that the first roughly 25 years of growth were excluded in order to eliminate a possible "juvenile effect" (McCarroll and Loader, 2004; Duffy et al., 2017). For each year, we pooled samples by species and status, with the exception of every 5th year, for which samples were separated by individual tree in order to preserve some measure of between-tree variability in isotope signal (Leavitt, 2010). Samples were homogenized and coarsely ground with a Wiley Mill (Thomas Scientific,

Swedesboro, NJ, USA), heat-sealed in commercial digestion pouches (ANKOM Technology, Macedon, NY, USA), and processed to remove extractives such as waxes, oils, and resins, which may be translocated across rings (Leavitt and Danzer, 1993; Harlow et al., 2006). Samples were then ground to a fine powder and weighed into tin capsules prior to analysis at Washington State University's Stable Isotope Core Laboratory (Pullman, WA, USA). Carbon isotope composition is expressed as the ratio of heavy (^{13}C) to light (^{12}C) carbon isotopes, relative to a standard, in "delta" notation (δ^{13}C). In order to account for changes in δ^{13}C due to increasing atmospheric CO_2 concentrations (c_a), we converted δ^{13}C to carbon isotope discrimination (Δ^{13}C) following (Farquhar et al., 1982; Farquhar and Richards, 1984):

$$\Delta^{13}C\ (\permil) = \frac{\left(\delta^{13}C_{air} - \delta^{13}C_{plant}\right)}{\left(1 + \dfrac{\delta^{13}C_{plant}}{1000}\right)} \tag{1}$$

Where $\delta^{13}C_{plant}$ is the carbon isotope signature of the wood, and $\delta^{13}C_{air}$ was determined from McCarroll and Loader (2004) and White et al. (2015). Δ^{13}C can also be related to the ratio of intercellular CO_2 (c_i) to c_a via:

$$\Delta^{13}C\ (\permil) \approx 4.4\permil + (27\permil - 4.4\permil)\frac{c_i}{c_a} \tag{2}$$

Where 4.4‰ and 27‰ are the fractionation constants due to diffusion through the stomata and fractionation due to Rubisco, respectively (Farquhar and Richards, 1984). Since Δ^{13}C is driven by the ratio of c_i to c_a, it is reflective of differences in stomatal conductance (g_s) and photosynthetic assimilation (A). For example, when g_s increases relative to A, the c_i/c_a ratio increases, which concurrently allows for greater "discrimination" against the heavier isotope (^{13}C) and higher Δ^{13}C. This scenario is typical of periods of minimal drought stress, whereas Δ^{13}C tends to decrease during periods of higher stress (Farquhar et al., 1989). Although it is generally assumed that variability in carbon isotope composition in wood is primarily driven by differences in discrimination against ^{13}C during diffusion through the stomata and photosynthesis, post-photosynthetic discrimination against ^{13}C may play a role in driving carbon isotope ratios, although the effect of these fractionating processes on carbon isotope ratios in extractive-free wood is not well understood (Gessler et al., 2014).

A subset of pinyon and ponderosa pines was additionally randomly selected from the group of successfully dated trees to assess resin ducts such that a total of 10 live and 10 dead trees were assessed for each pine species. Full methods of resin duct sampling are described in Hood et al., in review. We measured resin ducts from 1949-present in ImageJ (v. 1.46r, National Institutes of Health, Bethesda, MD, USA) and assigned the calendar year in which each duct formed. We followed the methods of Hood and Sala (2015) to calculate both unstandardized (mean resin duct size, number, total duct area) and standardized metrics (relative duct area, duct density) which utilize annual ring widths combined with the core width (4.5 mm) to determine ring area.

2.4. Analyses of surviving versus dying trees

2.4.1. Tree-level differences

Differences in tree diameter and height, as well as annual BAI (i.e. radial growth) and Δ^{13}C for live and dead trees were assessed via Student's t-test for each species. Time series of radial growth and Δ^{13}C were not detrended for these analyses to preserve any differences in long-term trends between live and dead trees. In order to understand the relationship of Δ^{13}C and radial growth, mean annual values of radial growth were regressed with mean Δ^{13}C across the study period. Both BAI and Δ^{13}C were detrended for this analysis using a spline method to remove any influence of age-related trends. While we assessed differences in resin duct metrics between live and dead trees over the entire

study period, differences were most apparent within the 5-years prior (2007–2011) to the drought. Therefore, we calculated the mean 2007–2011 values of each resin duct metric by tree and assessed for differences between live and dead trees using t-tests. A significance level of $p < 0.05$ was used for all analyses.

2.4.2. Mortality models

We examined site, stand, and tree-level factors that affected the probability of tree mortality via species-specific mixed-effects logistic regression models. We did not intend the models to predict individual tree death, but rather to detect the factors that may predispose trees to death in the event of drought and bark beetle outbreaks. Individual tree status was modeled for all cored trees (> 12.7 cm DBH/DRC) and predictor variables included site, stand, and tree-level variables. Site-level variables included plot slope, plot elevation, and linearly-transformed plot aspect (Beers et al., 1966). Stand-level variables included plot conspecific basal area and trees per hectare and were calculated from plot-level tree data. Tree-level variables included DBH or DRC, height, radial growth (mean 1949–2016 BAI), and/or an approximation of tree age (innermost ring year). We did not include both innermost ring year and mean 1949–2016 BAI in the same model as these two variables were highly collinear. While we did preliminary model runs that included BAI over different time periods (e.g. 5, 10, 20 years pre-drought), we found BAI over the entire study period to consistently perform best in models across species (data not shown). Diameter and height were similarly not included in the same model as these predictors were highly collinear. Instead, both predictors were assessed and the one resulting in the better-fit model was chosen. Conspecific basal area (BA) was used to approximate species-specific competition and host availability for bark beetles, while trees per hectare (TPH) included trees of all species and is a measure of stand density. We chose this combination of stand density variables as they continually performed better in models than conspecific TPH and BA of all trees. BAI was normalized by tree BA prior to inclusion in models to address collinearity with diameter and height. Since models included only cored trees, we required models to include at least one of the tree ring variables (BAI or inner ring year). We did not include interactions in models to avoid issues with overfitting, given the low sample sizes for some tree species. In order to account for the spatial distribution of the data and avoid spatial autocorrelation, models included plot-cluster as a random effect on the intercept. Since plot locations were clustered across the landscape, we chose to include plot-cluster rather than plot as the random effect as there was often only one tree per plot included in a model. Predictors were scaled and centered for ease of effect size comparison prior to inclusion in models.

We assessed all combinations of predictor variables and selected the model for which the combination of predictor variables yielded the lowest AIC as the "best-fit" model (Table S2). Collinearity, assessed via variance inflation factors, was not observed in any of the best-fit models. Spatial autocorrelation of tree status for the residuals of the best-fit models was assessed via spline correlograms for distances up to 8000 m. Correlograms indicated no unexplained spatial autocorrelation, and, importantly, spatial autocorrelation did not decrease with distance for any model. Model adequacy was tested and confirmed via fitted vs simulated quantile-quantile plots and classification rates were determined by training the best-fit model on 50% of the data and using it to predict the other 50%. All analyses were performed in R 3.6.1 (R Core Team, 2019). The package GLMMadaptive (Rizopoulos, 2019) was used for logistic model fitting and model selection, and ncf (Bjornstad, 2019) was used for assessing spatial autocorrelation.

2.4.3. Growth, Δ^{13}C and resin duct-climate relationships

We used regional Palmer Drought Severity Index (PDSI) data, an estimate of relative dryness calculated from temperature and precipitation data where negative values indicate higher aridity, in conjunction

with more local station-level temperature, precipitation, and relative humidity data for radial growth, Δ^{13}C, and resin duct-climate analyses. Relative humidity data were used to calculate leaf to air vapor pressure deficit (VPD) for additional assessment of potential water stress. We chose PDSI as an assessment of regional drought stress as it is has effectively captured past multi-year regional droughts well in our study area and because it is a widely used and understood drought index in many tree ring studies. Regional PDSI data were obtained from California Division 5 climate dataset (https://www.ncdc.noaa.gov/cag/divisional/mapping) which uses station data from across a geographic region to calculate monthly values. Since more local station data were available for temperature, precipitation and VPD, we used data from the meteorological station closest to the sampling areas with records dating to 1949 (LP=Sandberg, CA; SNF=Fresno Yosemite International Airport, CA; https://www.ncdc.noaa.gov/cdo-web/datatools/findstation).

Relationships of monthly, summer (Jun-Sept), previous summer, and hydrological year (Oct of previous year-Sept of current year) climate variables with tree-ring variables (detrended radial growth, Δ^{13}C, and resin duct metrics) were assessed via Pearson's correlations (Table S3; Table S4; Table S5). Since hydrological year PDSI was most consistently significantly related to tree ring variables, only this variable was used for subsequent analyses. In order to assess differences in sensitivity to climate between live and dead trees we conducted 20-year moving window analyses of correlations between hydrological year PDSI and tree-ring variables for individual species over the study period. Moving window analyses were conducted using the R package treeclim (Zang and Biondi, 2015).

3. Results

3.1. Overall mortality

Over the course of sampling (2016–19), mortality remained fairly constant within the LP area (27–30%), but changed substantially within the SNF area (43–54%), particularly for ponderosa pine (78–92%). Mortality levels determined from 2015 ADS data that contributed to site selection increased considerably over subsequent years with very few plots having <5% mortality by the end of the sampling period. Mean plot-level mortality for individual species ranged from 30% for pinyon pine to 91% for ponderosa pine but varied considerably by plot (Table 1). Mortality attributed to host-specific beetles was high for pinyon pine (97%; pinyon ips), ponderosa pine (93%; western pine beetle), and white fir (91%; fir engraver beetle), and all cored trees had evidence of successful attack by primary bark beetles. There were a very small number of trees for each of these species for which mortality agent could not be identified, although it is possible that these trees were attacked, but with beetle galleries present higher on trees boles than could be feasibly searched from the ground. Mortality agents for all incense cedar were unknown or attributed to suppression.

3.2. Site and stand characteristics

Mortality models indicated that while a more southwestern plot aspect was a significant predictor of mortality for incense cedar, other site-level predictors were less important (Table 2). Plot slope was present as a predictor for three out of the four species, although not in consistent directions. Plot elevation was only included in the white fir model and was not significant. Predictors related to stand characteristics (conspecific BA) were included in both ponderosa pine and white fir best-fit models, with trees from plots with higher conspecific BA having a higher probability of mortality. Conspecific BA was not included in models for any other species, and TPH was not included in any of the mortality models (Table 2).

3.3. Radial growth and tree size

When all trees, both cored and non-cored, were considered, few differences in diameter (DRC or DBH) or height between live and dead trees were observed (Table 1). Diameter was larger for pinyon pine that died, while height was shorter for incense cedar that died. No differences in size existed for either white fir or ponderosa pine (Table 1). When cored trees alone were considered in mortality models, only height differences remained important for incense cedar mortality probability (Table 2).

Differences in radial growth between surviving and dying trees were only apparent for ponderosa pine and incense cedar (Table 2; Fig. 2A; Fig. S1). Ponderosa pine that survived tended to have lower BAI than trees that died until around the time of the late 1980s-early 1990s, a time period corresponding to a multi-year regional drought and bark beetle outbreaks (Ferrell et al., 1994; Goulden and Bales, 2019), at which point growth differences between dying and surviving trees decreased (Fig. 2A). In contrast, BAI of incense cedar that survived tended to be higher than for trees that died throughout the study period, and particularly in recent decades. Although radial growth was not a predictor in the incense cedar mortality model, inner ring year (a proxy for tree age) was (Table 2), which is highly related to mean radial growth over the study period ($r = 0.67$). While radial growth of white fir that survived tended to be lower than of those that died for much of the study period, these differences were not significant, and BAI was not a significant predictor in the best-fit white fir logistic regression model (Table 2; Fig. 2A). Differences between surviving and dying pinyon pine were virtually nonexistent throughout the entire study period (Fig. 2A).

3.4. Carbon isotopes and Δ^{13}C-BAI relationships

Across species, differences in carbon isotope discrimination (Δ^{13}C) between live and dead trees were not consistent (Fig. 2B; Fig. S2). Ponderosa pine that survived had higher Δ^{13}C throughout most of the study period than trees that died. Pinyon pine and white fir that survived also tended to have higher Δ^{13}C, but those differences were weak

Table 1
Tree counts (≥ 12.7 cm), mean diameters (DBH/DRC; cm), mean height (m) and percent dead by species based on 2018 data across all plots. Percent dead includes plot-level ranges, and diameter and height include 1 S.E. in parentheses. Differences were assessed via *t*-test with bold type indicative of significance ($p < 0.05$).

	Pinyon pine		Ponderosa pine		White fir		Incense cedar	
	Live	Dead	Live	Dead	Live	Dead	Live	Dead
All trees/all plots								
Count	310	132	18	181	151	118	118	66
DBH/DRC	**26.3 (0.6)**	**30.9 (0.9)**	41.1 (6.9)	40.4 (1.7)	39.2 (1.9)	40.7 (2.5)	31.9 (2.4)	31.1 (2.2)
Height	8.5 (0.4)	9.1 (0.5)	19.5 (3.2)	20.9 (0.8)	20.3 (0.9)	20.2 (1.1)	**14.0 (0.8)**	**11.0 (0.8)**
Dead (%)	30 (0–81)		91 (0−100)		45 (0–100)		36 (0–74)	
Cored trees								
Count	42	21	11	38	36	31	30	18
DBH/DRC	28.2 (1.6)	30.2 (1.9)	57.5 (8.1)	58.2 (4.0)	49.4 (3.8)	63.8 (11.2)	39.9 (4.2)	33.9 (4.4)
Height	8.5 (0.4)	9.1 (0.5)	26.6 (4.1)	30.4 (5.2)	28.3 (2.8)	27.3 (3.0)	17.5 (1.6)	13.4 (1.8)

Table 2
Model coefficients and classification rates for best-fit logistic regression models of mortality by species[a].

Species	Intercept	DBH/DRC	Height	BAI	Inner ring year	Plot slope	Plot elevation	Plot aspect	Plot consp. BA	Plot TPH	Class. rate
Pinyon pine	**−0.84**	–		**−0.62**	–	0.23	–	–	–	–	0.72
Ponderosa pine	**2.43**	–		**1.8**	–	−0.89	–	–	**2.79**	–	0.88
White fir	−0.33		–	0.32	–	0.53	−0.64	–	**0.94**	–	0.61
Incense cedar	**−0.82**		**−1.63**		**−1.94**	–	–	**−1.19**	–	–	0.75

[a] Predictors were scaled and centered prior to model fitting for ease of effect size comparison. BAI was additionally normalized by BA to eliminate possible collinearity issues. Rows correspond to individual models. Bold indicates significance of a predictor ($p < 0.05$), and dashed lines indicate predictor was included in model selection, but did not appear in best-fit model. Classification rates were determined by training the model on 50% of the data and using that to predict the other 50%.

and not significant. Incense cedar showed inconsistent differences between live and dead trees throughout the study period (Fig. 2B).

Relationships between radial growth and Δ^{13}C were all positive and significant but differed in strength across species and tree status (Fig. 3). Pinyon pine had a strong, positive correlation between radial growth and Δ^{13}C for both surviving and now-dead trees. Similarly, ponderosa pine that died had a relatively strong, positive correlation between growth and Δ^{13}C, while a weaker relationship existed between the two variables for trees that survived. The BAI- Δ^{13}C relationship for surviving and dying white fir and incense cedar was weakly positive, yet statistically significant (Fig. 3).

3.5. Defenses

In general, there were no clear differences in resin duct metrics between live and dead pinyon and ponderosa pines when the whole

Fig. 2. Differences in basal area increment (BAI) and isotopic discrimination against ^{13}C (Δ^{13}C) between live and dead trees of each study species. Positive differences indicate higher growth (A) or discrimination (B) of trees that survived the drought and bark beetle outbreaks relative to trees that died. Open circles denote significant differences ($p < 0.05$).

study period was considered (Fig. S4). However, in the 5 years leading up to the 2012–2016 drought some differences emerged (Fig. 4). Surviving ponderosa pines had higher relative duct area, and weakly greater duct density ($p < 0.1$). Pinyon pines that survived had greater duct production (i.e. number of ducts), and weakly higher total duct area ($p < 0.1$; Fig. 4).

3.6. Relationships of tree-ring variables to climate

3.6.1. Radial growth and climate

Correlations of radial growth with hydrological year PDSI were nearly always positive across the study period but varied in strength by species and tree status (Fig. 5). Only ponderosa pine showed consistent differences in growth sensitivity to PDSI for live and dead trees, with those that died having a consistently higher correlation with PDSI than those that survived. Correlations between incense cedar growth and PDSI were typically not significant over the study period, and varied minimally between live and dead trees, with the exception of a more pronounced decline in sensitivity to PDSI around the 1980s-early 1990s for trees that eventually died (Fig. 5).

3.6.2. Δ^{13}C and climate

Similar to growth, correlations of Δ^{13}C with hydrological year PDSI were nearly always positive but varied in strength by species and tree status (Fig. 6). With the exception of incense cedar, sensitivity of Δ^{13}C to PDSI seemed to decline over the study period. Incense cedar that died had relatively invariable Δ^{13}C-PDSI relationships, and trees that survived seemed to become more sensitive to PDSI over the time frame measured. Interestingly, although live and dead pinyon pine had similar Δ^{13}C-PDSI relationships over much of the study period, Δ^{13}C of dead trees appears to become less sensitive to PDSI in recent decades while it remained relatively constant for trees that survived. While differences in sensitivity of Δ^{13}C to PDSI are less consistent for ponderosa pine or white fir, ponderosa pine Δ^{13}C-PDSI correlations of dead trees seem to have declined faster in recent decades, and correlations for dead white fir tended to be higher than for live individuals (Fig. 6).

3.6.3. Defenses and sensitivity to climate

Correlations of resin duct metrics with PDSI were similar for both live and dead pinyon pine, whereas ponderosa pine that died had generally stronger correlations between duct metrics and PDSI than surviving trees (Fig. 7). Relationships between unstandardized resin duct metrics of dead ponderosa pine and PDSI tended to become increasingly positive over the study period. Conversely, sensitivity of all duct metrics to PDSI for live trees appears to have declined particularly in recent decades (Fig. 7).

4. Discussion

We find a unique suite of risk factors for mortality for pinyon pine, ponderosa pine, white fir, and incense cedar, with few risk factors shared between species, and no generalizable predictors of mortality across all four species (Fig. 8). We find that in the face of a particularly
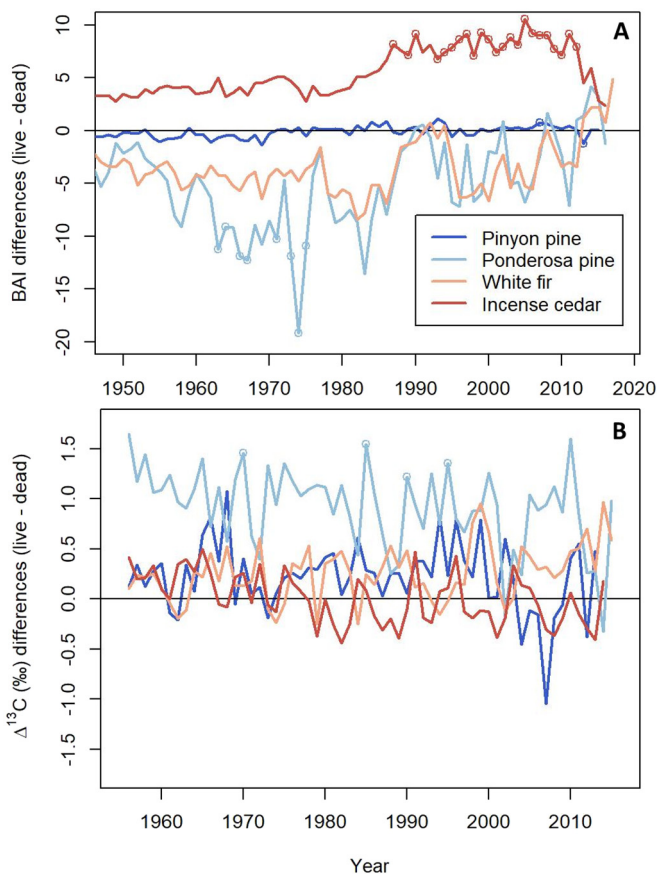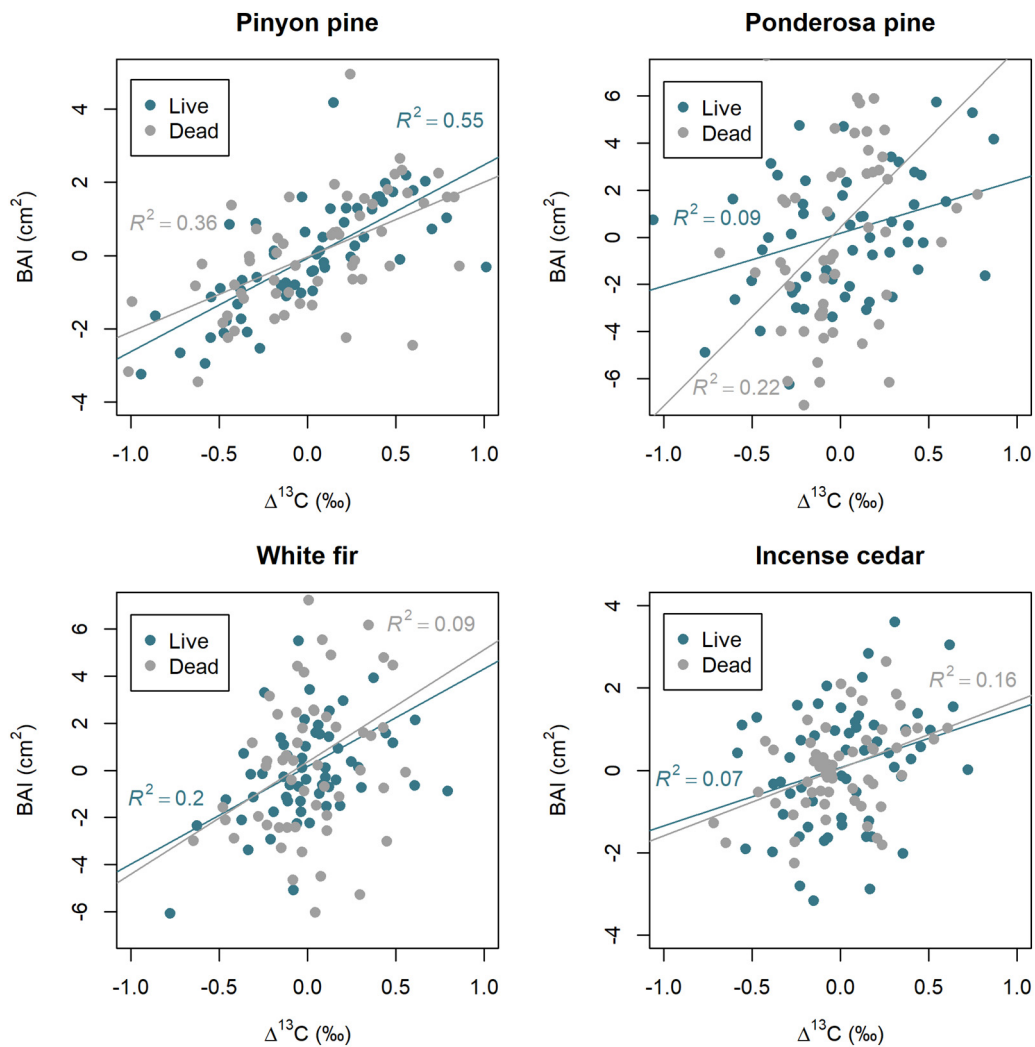
Fig. 3. Detrended basal area increment (BAI) vs detrended discrimination (Δ^{13}C) for live and dead trees with adjusted-R^2 values. All correlations are significant ($p < 0.05$).

long, hot drought combined with bark beetle outbreaks, tree-level factors previously found to affect susceptibility to either drought alone or beetle outbreaks combined with more moderate drought become less clear. Our findings support the premise that species' responses to drought stress, particularly when severe drought or beetles are involved are highly plastic and may depend on species- or even site-specific risk factors (Cailleret et al., 2017; Gessler et al., 2018; Zadworny et al., 2019).

4.1. Stand structure matters for some species

As anticipated, differences in stand structure influenced mortality probability, but only for ponderosa pine and white fir, and tree density alone was not important (Table 2). Ponderosa pine and white fir that came from plots with higher conspecific BA had a higher probability of mortality, which is generally consistent with studies that examined mortality factors during both the 2012–2016 California drought (Restaino et al., 2019) and a previous drought-related beetle outbreak (Ferrell et al., 1994; Egan et al., 2010). This pattern is likely related to the importance of host-tree abundance for beetle success and/or a competition effect.

Surprisingly, site-level variables related to water availability like elevation or aspect did not appear to be of much importance in predicting mortality in our models. Incense cedar that died were more likely to come from plots on more southwestern aspects, and white fir was the only species for which elevation showed up as a predictor in the best-

fit model, although it was non-significant (Table 2). Other studies that have examined mortality factors associated with the recent California drought have found elevation, which is strongly associated with water availability in the Sierra Nevada, to play an important role in mortality (Paz-Kagan et al., 2017; Fettig et al., 2019; Goulden and Bales, 2019; Restaino et al., 2019). Our study design did not aim to stratify plots across the elevational range of the study species and it is likely that our study area did not have a sufficient distribution of plots across a large enough elevational range to adequately capture this more landscape-level risk factor.

4.2. Differences in radial growth and tree size

Radial growth and tree diameter are two commonly assessed tree-level variables in studies that compare trees that die and those that survive drought and/or bark beetle outbreaks. A recent extensive synthesis of radial growth patterns preceding drought-related mortality showed that while trees that die during drought alone generally have lower growth rates prior to death, this pattern does not necessarily hold true for trees that die from bark beetles or from particularly severe drought (Cailleret et al., 2017). Our findings support this, with incense cedar being the only species of the four we examined where chronically slower growth preceded death, and for which we did not observe clear bark beetle-related mortality. In contrast to the other species we studied, incense cedar mortality appears to be more attributable to
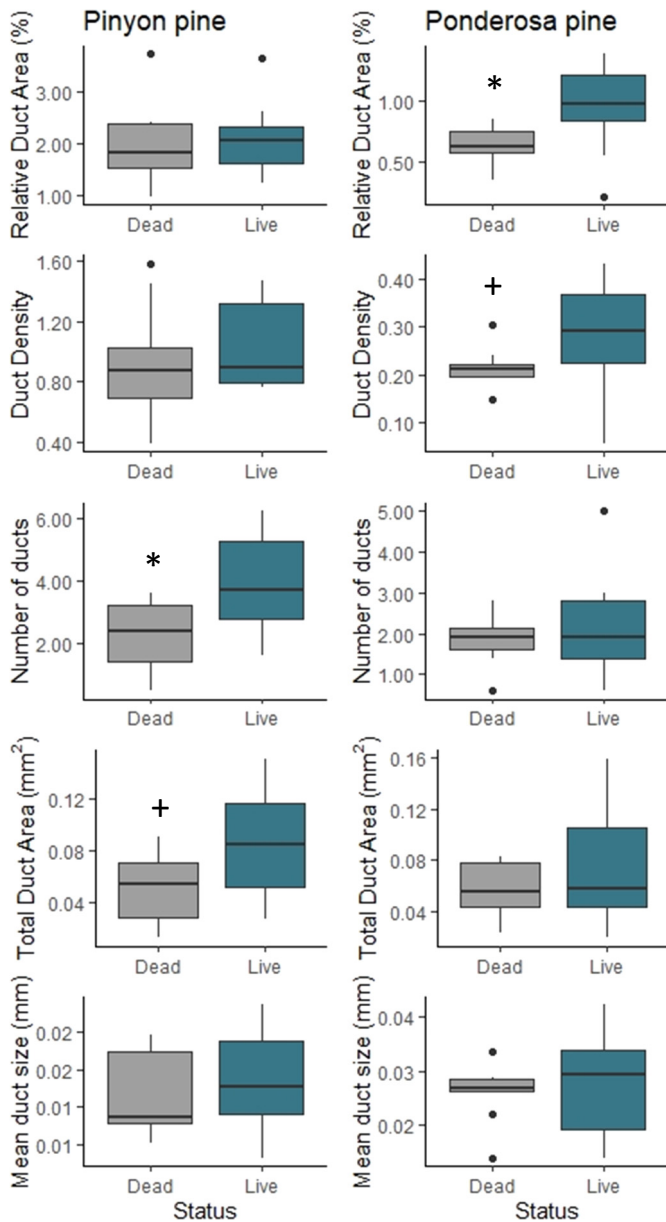
Fig. 4. Resin duct variables measured over the five years prior to the drought (2007–2011) for live and dead trees. * indicates significance ($p < 0.05$); + indicates $p < 0.1$.

suppression, or perhaps a combination of cedar bark beetle selection of smaller trees (Stephenson et al., 2019), with the competitive advantage of taller and faster growing trees over shorter, slower growing individuals. Consistent with this observation, Fettig et al. (2019) also attributed the majority of incense cedar mortality in the central and southern Sierra during the recent drought to suppression rather than beetle-related mortality.

Trees that die due to beetles alone or in combination with more moderate drought often have chronically higher growth, possibly due to growth-defense tradeoffs or beetle selection during extended outbreaks for larger trees (Ferrenberg et al., 2014; de la Mata et al., 2017; Cooper et al., 2018; Kichas et al., 2020). We similarly observe this trend for ponderosa pine and weakly for white fir that died, suggesting that the effects of bark beetles may have overridden the effects of the drought for these species. However, our study design did not allow us to examine the influence of drought and bark beetles separately because nearly all dead trees showed signs of attack by a primary beetle. This is a

common challenge in mortality studies involving biotic agents because drought also influences bark beetle populations (Anderegg et al., 2015). Generally though, the lack of differences in growth in the years immediately preceding death for ponderosa pine and white fir, and the lack of growth differences over the entire period for pinyon pine (Fig. 2A), suggests that when beetles occur in concert with a particularly extreme drought, growth differences alone are not sufficient predictors of mortality.

Surprisingly, differences in diameter between surviving and dying trees were only observed for pinyon pine, with trees that died tending to be larger (Table 1). Consistent with our results, Meddens et al. (2015) found the main factor to reliably differ between live and dead two-needle pinyon pine (*Pinus edulis* Engelm.) affected by the combination of drought and pinyon ips outbreaks to be diameter, with larger trees more likely to die. This could be due to a preference of bark beetles for larger trees, a tendency of larger trees to have greater metabolic demands, or a prioritization of growth over investment in defenses (Meddens et al., 2015). While diameter was important when considering both cored and non-cored trees, it was not included in the best-fit model for pinyon pine (Table 2), and it is possible that this inconsistency is attributable to sample size.

4.3. Long-term variability in carbon isotope patterns may play role in ponderosa pine mortality susceptibility

Long-term variability in $\Delta^{13}C$ between surviving and dying trees is indicative of chronic differences in intrinsic water-use efficiency (iWUE; A/g_s; McCarroll and Loader, 2004), and possibly water stress (Warren et al., 2001). Only ponderosa pine exhibited differences in $\Delta^{13}C$, with trees that died having consistently lower $\Delta^{13}C$ than those that survived (Fig. 2B). Lower $\Delta^{13}C$ typically results from either reduced stomatal conductance, greater photosynthetic demand, or some combination of the two (i.e. higher iWUE). However, it is additionally possible that post-photosynthesis fractionation processes, particularly due to the utilization of stored assimilates, could contribute to some of the $\Delta^{13}C$ patterns we observe (Gessler et al., 2014). Consistently higher BAI of now-dead ponderosa pine over much of the same time period suggests that lower $\Delta^{13}C$ may be due in part to chronically higher photosynthetic demand linked to higher growth, rather than chronic differences in stomatal conductance driven by long-term water stress.

Although chronic differences in BAI and $\Delta^{13}C$ suggest long-term differences in photosynthetic demand between surviving and dying ponderosa pine, variability in the strength of the relationship between BAI and $\Delta^{13}C$ suggests that drivers may differ when examined on an interannual basis. The strength of the relationship between intrinsic water-use efficiency, which is inversely related to $\Delta^{13}C$, and radial growth has been shown to differ between trees that survive and those that die as a result of drought or drought-induced beetle-related mortality, with a tighter coupling observed for trees that eventually die (McDowell et al., 2010; Voltas et al., 2013; but see Hereş et al., 2014). This is consistent with our results for ponderosa pine (Fig. 3). This relationship when combined with the stronger relationship between BAI and PDSI for now-dead ponderosa pine, indicates that at least interannually, years in which $\Delta^{13}C$ was lower and drought more intense, trees that eventually died had less radial growth. This suggests that interannual variability in $\Delta^{13}C$ of now-dead trees may be more tightly linked to differences in stomatal conductance rather than photosynthetic demand. Although $\Delta^{13}C$ differences between surviving and dying trees were negligible for other species, we do observe that radial growth of pinyon pine is particularly tightly related to $\Delta^{13}C$ for both live and dead trees. This is perhaps unsurprising as pinyon pine additionally had chronically low growth and low $\Delta^{13}C$ (Fig. S1; Fig. S2), and is growing at the southern and lower elevational extent of its range (i.e. more water-limited), consistent with the notion that these trees are living under more chronically stressed conditions. These conditions could make radial growth more sensitive to changes in $\Delta^{13}C$, particularly if
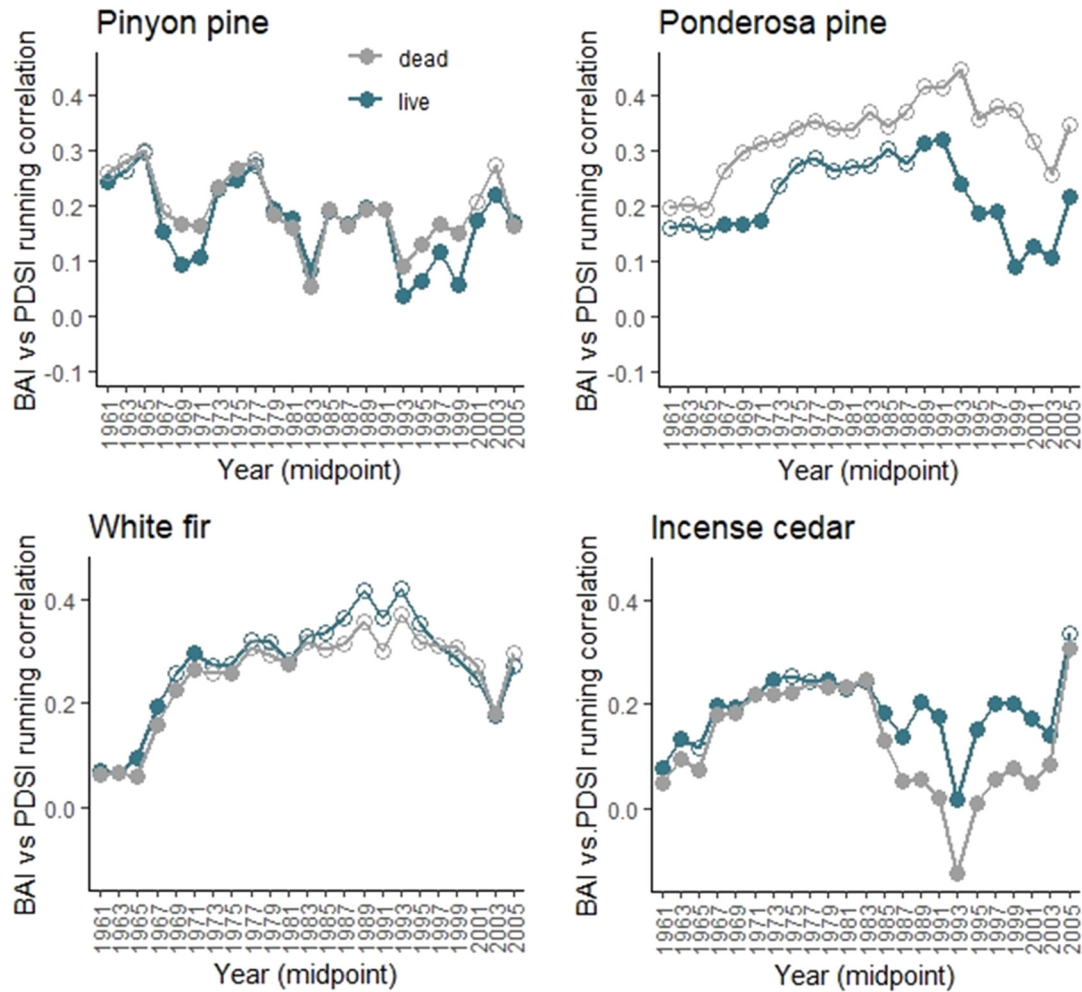
Fig. 5. Basal area increment (BAI) vs hydrological year Palmer Drought Severity Index (PDSI) 20-year moving window correlation coefficients for live and dead trees. BAI is detrended. Open circles indicate significant correlation of BAI vs PDSI ($p < 0.05$). Years are midpoints of 20-year moving windows; moving windows are offset by two years.

those changes are driven primarily by variability in stomatal conductance. The lack of variability of $\Delta^{13}C$ or the BAI-$\Delta^{13}C$ relationships or between surviving and dying white fir and incense cedar suggests that growth sensitivity to changes in stomatal conductance and/or photosynthetic demand was not a driving factor in mortality risk for either of these species (Fig. 3).

4.4. Influence of beetle dynamics and role of defenses

Bark beetle dynamics may change over the course of an outbreak, particularly when paired with an ongoing drought, thereby differentially influencing the mortality probability of some trees over others during the course of an outbreak (Boone et al., 2011; Egan et al., 2016; de la Mata et al., 2017). Beetle dynamics likely influenced the higher probability of mortality for larger pinyon pine (Negrón and Wilson, 2003), as well as the greater likelihood of mortality for ponderosa pine and white fir growing in areas with higher conspecific basal area. Forests with more and larger hosts can foster increases in beetle populations by making it easier for beetles to find host trees through pheromone-mediated communication and higher brood production (Egan et al., 2010, Raffa, 2014). Although beetles may have initially attacked smaller individuals, the length of the drought and thus the continued and increased beetle pressure likely allowed for successful attacks of larger individuals as well, as has been observed for other pines (Boone et al., 2011; Egan et al., 2016; de la Mata et al., 2017; Cooper et al., 2018).

Water stress can predispose ponderosa pine to attack from bark beetles via decreases in defenses, particularly resin flow (Kolb et al., 2019) and resin ducts (Gaylord et al., 2013). Although we do not assess resin flow directly, resin duct metrics, particularly unstandardized metrics, are highly related to resin flow (Hood and Sala, 2015). In our study, only relative duct area for ponderosa pine and duct number for pinyon pine were higher for surviving trees compared to trees that died (Fig. 4). Studies that have examined differences in resin duct metrics in two-needle pinyon pine have primarily found smaller ducts in the years preceding drought and beetle induced mortality (Gaylord et al., 2013; Gaylord et al., 2015), a trend we similarly observe, although nonsignificantly (Fig. 4). Differences have likewise been found in resin duct metrics between surviving and dying ponderosa pine (Kane and Kolb, 2010; Hood et al., 2015), although differences have typically been associated with unstandardized metrics, rather than those standardized by ring area as we observed. It is possible that the drought and resulting bark beetle outbreak were so severe that trees were greatly constrained from producing both constitutive and induced resin and resin ducts. This constraint combined with high beetle pressure may have masked differences in resin ducts between resistant and susceptible trees that exist under milder climatic conditions. It is important to note that we only assess one component of tree defense to bark beetles, and other factors, such as chemical composition of resin and induced responses, are additionally important for tree defense (Raffa, 2014; Huang et al., 2020).

The prolonged drought likely negatively impacted tree defenses, which together with high host availability, supported conditions for
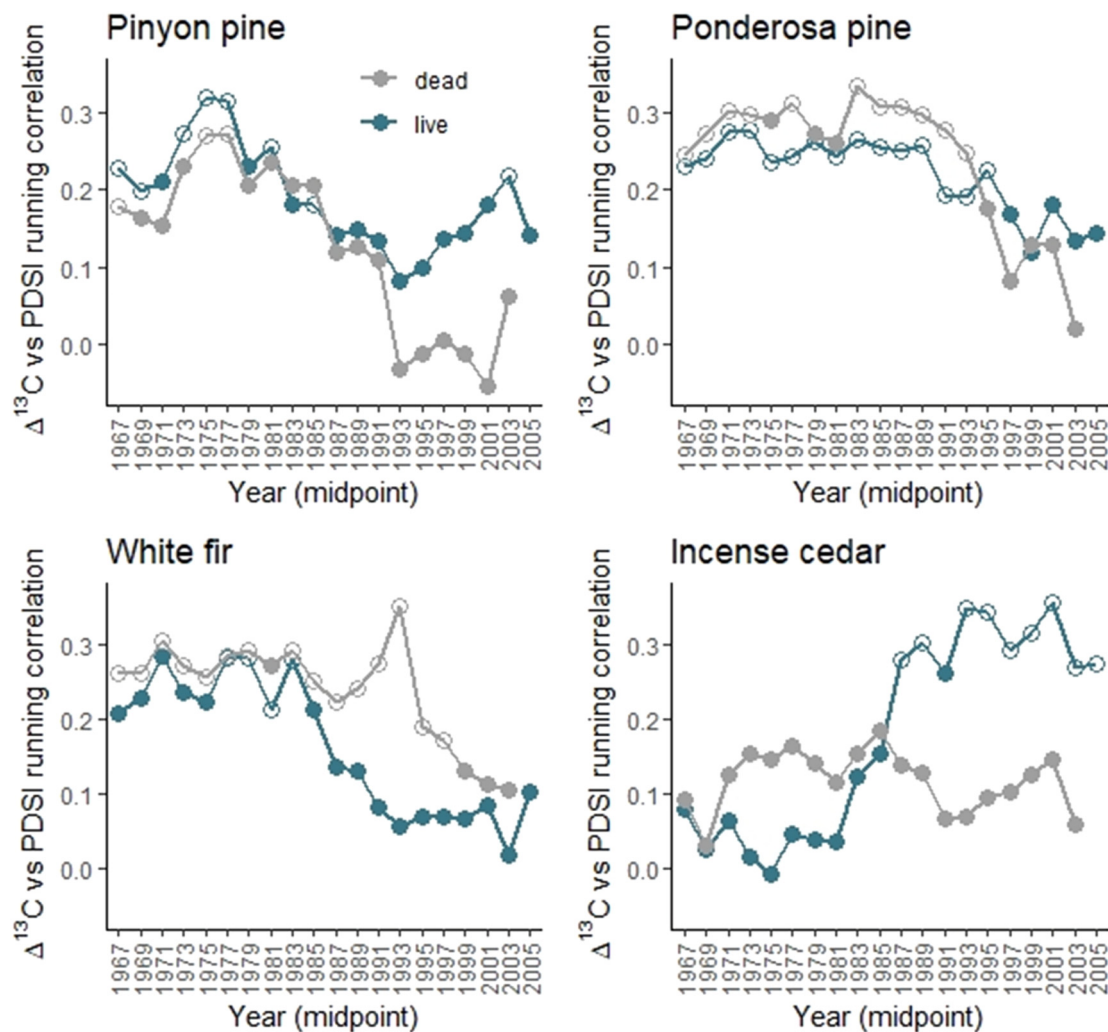
Fig. 6. Discrimination ($\Delta^{13}C$) vs hydrological year Palmer Drought Severity Index (PDSI) 20-year moving window correlation coefficients for live and dead trees. $\Delta^{13}C$ is detrended. Open circles indicate significant correlation of $\Delta^{13}C$ vs PDSI ($p < 0.05$). Years are midpoints of 20-year moving windows; moving windows are offset by two years.

extended, severe beetle outbreaks. The effectiveness of tree defenses changes with beetle population dynamics, with bark beetles during an outbreak preferentially attacking better defended trees (Boone et al., 2011). While seemly counter-intuitive, it is likely due to higher beetle fitness in larger trees that can support greater brood size and increase reproductive output. Therefore, tree defenses may become less effective as beetle populations build and are capable of overwhelming defenses (Raffa, 2014) because the conditions needed to support an outbreak are different than the ones required to initiate it (Raffa et al., 2008). While defenses still influence beetle attack success, forest structure and host tree abundance may become increasingly important as an outbreak progresses (Fettig et al., 2019; Fettig et al., 2007; Hood et al., 2016).

4.5. Greater sensitivity to climate for dead trees of some species but not others

Greater sensitivity of growth to climate has been found to be more pronounced in trees that succumb to drought with or without a concurrent beetle outbreak (McDowell et al., 2010; Hereş et al., 2012; Cooper et al., 2018), and in some cases this greater sensitivity also holds true for carbon isotopes (Voltas et al., 2013; Csank et al., 2016). In contrast to our expectations, ponderosa pine was the only species that showed consistently greater growth sensitivity to PDSI throughout the study

period for trees that died (Fig. 5), suggesting a long-term greater sensitivity to water stress which may have contributed to mortality for this species.

Differences between live and dead trees were more apparent in the sensitivity of $\Delta^{13}C$ to PDSI, predominantly in the two decades prior to the drought, with live pinyon pine in particular having relatively stronger correlations than trees that died (Fig. 6). This result is consistent with observations for ponderosa pine growing at water-limited sites (McDowell et al., 2010). A weaker or more strongly declining relationship of $\Delta^{13}C$ to drought suggests that dying trees may have had less stomatal sensitivity to drought thereby inhibiting the adaptive response of increasing their water-use efficiency as strongly during drought periods. In contrast, the slightly stronger relationship between $\Delta^{13}C$-PDSI for dying white fir is more consistent with observations for white spruce (Csank et al., 2016), and suggests that trees that eventually died had a greater stomatal sensitivity to drought in the years preceding death. For incense cedar, the $\Delta^{13}C$-PDSI relationship remained weak over time for trees that died, whereas it became stronger for surviving trees (Fig. 6). If incense cedar that died are being outcompeted by faster growing, taller trees, it follows that their stomatal sensitivity and/or photosynthetic demand, both of which determine $\Delta^{13}C$, may be less coupled with climate and more linked to site-level resource dynamics (e.g. light, nutrient availability). Weaker growth-climate relationships have been previously observed for suppressed individuals when compared to more dominant

trees (Martín-Benito et al., 2008; Lebourgeois et al., 2014), which is generally consistent with our observations for incense cedar in recent decades and appears to hold true for Δ^{13}C-drought relationships as well (Fig. 5; Fig. 6). We additionally note that many of the shifts in sensitivity of both radial growth and Δ^{13}C to PDSI that we observe appear to correspond with the multi-year regional drought and bark beetle outbreaks that occurred in the late 1980s-early 1990s. There is some evidence that previous droughts may influence susceptibility of trees to future droughts (Macalady and Bugmann, 2014), particularly if drought stress is severe enough to cause long-term harm to photosynthetic

machinery or hydraulic function. It is possible that this past drought catalyzed changes in relationships of radial growth or Δ^{13}C with PDSI and may help to explain some of the shifts that we observe.

Relationships between resin duct metrics and drought indicate that ponderosa pine that died had consistently greater sensitivity of resin duct size, number and area to drought, whereas differences between surviving and dying pinyon pine were inconsistent (Fig. 7). This suggests that chronic sensitivity to water stress in dying ponderosa pine may have impacted defenses during periods of drought, thereby increasing susceptibility to bark beetle attack.
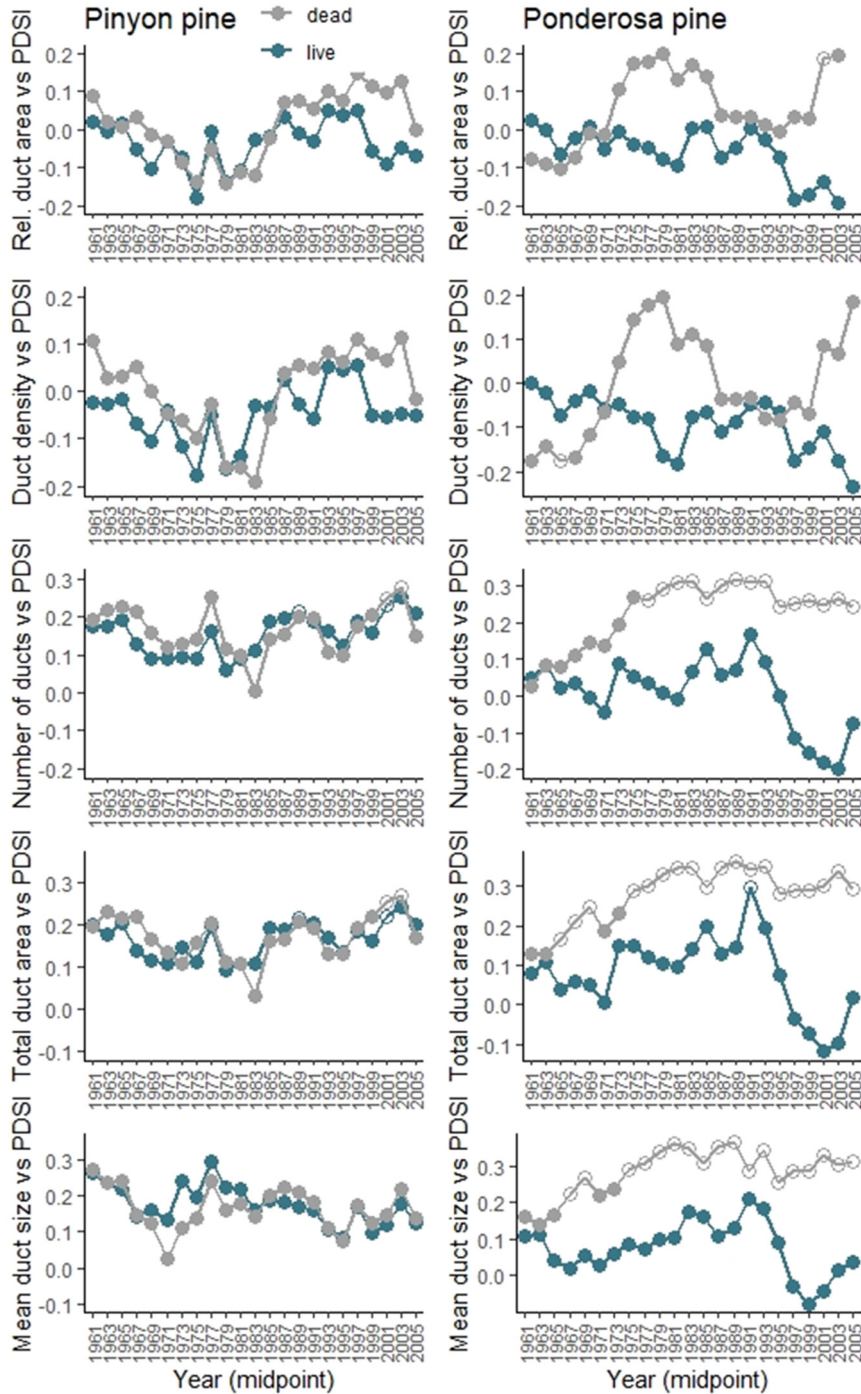

Fig. 7. Resin duct metrics vs hydrological year (Oct-Sept) Palmer Drought Severity Index (PDSI) 20-year moving window correlation coefficients for live and dead trees. Open circles indicate significant correlation of duct size vs PDSI ($p < 0.05$). Years are midpoints of 20-year moving windows; moving windows are offset by two years.

4.6. Considering mechanisms of mortality

Although we do not attempt to explicitly determine mortality mechanisms, the variability we see across species in the physiological, climatological and beetle-related factors influencing mortality probability suggests that mechanisms may vary between species. Current understanding of drought-related mortality mechanisms suggests the combined importance of tree carbon budget and the hydraulic system (Adams et al., 2017), both of which are impacted by bark beetles via a depletion of carbon reserves for tree defenses and via beetle-associated fungi blocking water transport in the xylem (Anderegg et al., 2015). We expect that mortality mechanisms related to both the hydraulic system and carbon budget interact in the face of such a severe disturbance, as has been demonstrated in other systems (Sevanto et al., 2014; Gaylord et al., 2015). For example, the steep decline in $\Delta^{13}C$ sensitivity to climate in the years preceding the drought we observe for ponderosa pine that died may point to a lack of stomatal control which could result in failure of the hydraulic system. In contrast, a greater investment in growth for dead ponderosa pine over the study period combined with less investment in defenses in the years preceding the drought, suggests a riskier strategy of growth prioritization that could lead to carbon starvation-related mortality in the face of a multi-year drought and bark beetle outbreak (McDowell et al., 2008).

4.7. Other considerations

There are additional considerations we did not address that may play equally important roles in influencing mortality susceptibility of some trees over others. For example, we did not attempt to quantify belowground processes that may influence access to resources. Changes in root-to-shoot ratios, fine root abundance and distribution, and mycorrhizal networks may alter a tree's ability to withstand drought (Mohan et al., 2014; Brunner et al., 2015). Similarly, differences in rooting depth or soil water holding capacity due to microsite characteristics may influence tree-level differences in water availability and could help to further explain within-species differences in ability to withstand both drought and bark beetle outbreaks. A better understanding of how belowground factors vary both among and within species in the face of drought and concurrent bark beetle outbreaks is necessary to better model tree-level mortality and is an area in which further research is much needed (Phillips et al., 2016). Other physiological indicators of tree stress and vulnerability to drought such as non-structural carbohydrates and water content (Martínez-Vilalta et al., 2016; Lehmann et al., 2018; Sapes et al., 2019) were similarly outside the scope of this project. Lastly, variability between trees that survive and those that die from the combination of drought and concurrent beetle outbreaks may in part be due to genetic differences between trees (Sthultz et al., 2009; de la Mata et al., 2017), and should be considered when modeling future tree mortality in the face of extreme disturbance events.

5. Conclusions

The predicted increase in the intensity and/or length of droughts globally (IPCC, 2014; Trenberth et al., 2014), combined with changes in bark beetle dynamics associated with climate change (Bentz et al., 2010), requires a better understanding of how severe disturbance events influence mortality at the tree-level if we are to effectively predict future forest mortality. We find that risk factors associated with tree-level mortality differ between species, and that generalizable patterns become less clear when bark beetle outbreaks occur in concert with a particularly long, hot drought, likely a reflection of unique strategies for dealing with these specific types of disturbance (Fig. 8). For ponderosa pine, we see evidence that both long-term differences in chronic demand of carbon for growth and sensitivity to water stress
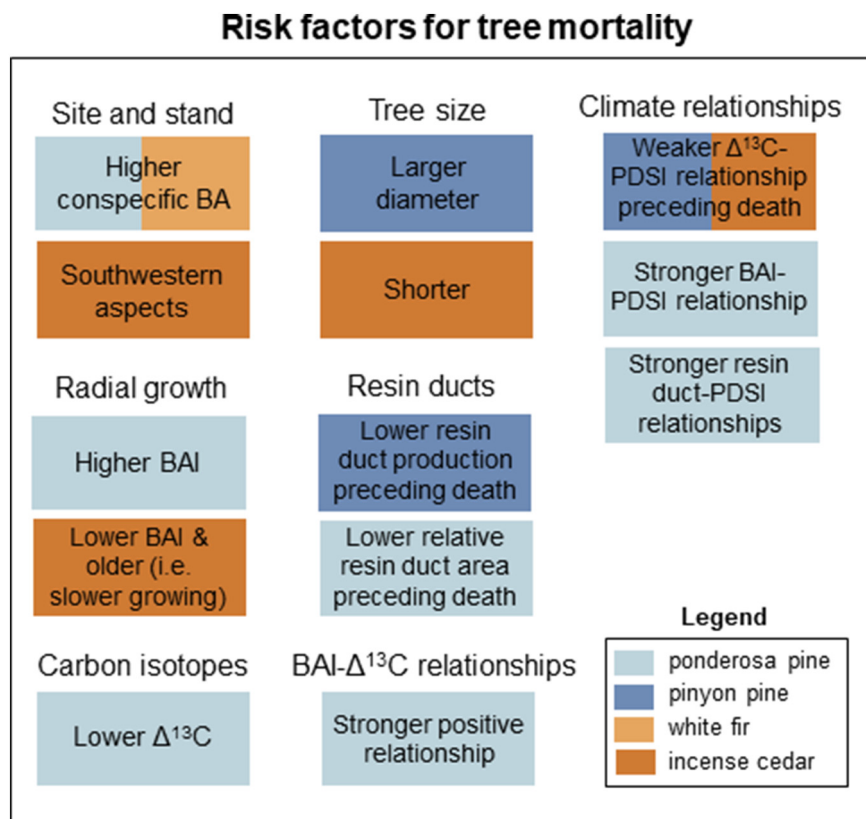

Fig. 8. Identified within-species risk factors for tree-level mortality due to severe drought and concurrent bark beetle outbreaks. Risk factors are categorized by species and category of metric measured.

combine with shorter term beetle-related selection and variability in defenses to influence susceptibility to the combination of drought and beetle attacks. Whereas for pinyon pine and white fir, long-term variability between trees that survived and those that died is less clear and beetle dynamics may play a more prominent role in mortality patterns. Incense cedar, in contrast, for which we see limited evidence of beetle-related mortality, appears to be primarily influenced by long-term differences in growth rate and stand dominance which likely impact resource availability and susceptibility to prolonged drought. Models that aim to predict tree-level mortality under future climate scenarios will need to account for these extreme events, and may need to consider multiple species-specific risk factors to more accurately predict tree death. Further study of these types of droughts will be necessary if we are to accurately forecast forest mortality in the face of future droughts of similar magnitude.

CRediT authorship contribution statement

Charlotte C. Reed: Investigation, Formal analysis, Data curation, Visualization, Writing - original draft. **Sharon M. Hood:** Conceptualization, Methodology, Investigation, Writing - review & editing.

Declaration of competing interest

The authors declare that they have no known competing financial interests or personal relationships that could have appeared to influence the work reported in this paper.

Acknowledgements

Data availability

All tree ring data have been archived in the International Tree-Ring Databank (ITRDB) and are available online (https://www.ncdc.noaa.gov/paleo-search/).

Appendix A. Supplementary data

Supplementary data to this article can be found online at https://doi.org/10.1016/j.scitotenv.2020.141306.

References

Adams, H.D., Zeppel, M.J., Anderegg, W.R., Hartmann, H., Landhäusser, S.M., Tissue, D.T., Huxman, T.E., Hudson, P.J., Franz, T.E., Allen, C.D., 2017. A multi-species synthesis of physiological mechanisms in drought-induced tree mortality. Nature ecology & evolution 1, 1285. https://doi.org/10.1038/s41559-017-0248-x.

Allen, C.D., Macalady, A.K., Chenchouni, H., Bachelet, D., McDowell, N., Vennetier, M., Kitzberger, T., Rigling, A., Breshears, D.D., Hogg, E.H., Gonzalez, P., Fensham, R., Zhang, Z., Castro, J., Demidova, N., Lim, J.-H., Allard, G., Running, S.W., Semerci, A., Cobb, N., 2010. A global overview of drought and heat-induced tree mortality reveals emerging climate change risks for forests. For. Ecol. Manag. 259, 660–684. https://doi.org/10.1016/j.foreco.2009.09.001.

Allen, C.D., Breshears, D.D., McDowell, N.G., 2015. On underestimation of global vulnerability to tree mortality and forest die-off from hotter drought in the Anthropocene. Ecosphere 6, 129. https://doi.org/10.1890/ES15-00203.1.

Anderegg, W.R.L., Hicke, J.A., Fisher, R.A., Allen, C.D., Aukema, J., Bentz, B., Hood, S., Lichstein, J.W., Macalady, A.K., McDowell, N., Pan, Y., Raffa, K., Sala, A., Shaw, J.D., Stephenson, N.L., Tague, C., Zeppel, M., 2015. Tree mortality from drought, insects, and their interactions in a changing climate. New Phytol. 208, 674–683. https://doi.org/10.1111/nph.13477.

Beers, T.W., Dress, P.E., Wensel, L.C., 1966. Notes and observations: aspect transformation in site productivity research. J. For. 64, 691–692.

Bentz, B.J., Regniere, J., Fettig, C.J., Hansen, E.M., Hayes, J.L., Hicke, J.A., Kelsey, R.G., Negron, J.F., Seybold, S.J., 2010. Climate change and bark beetles of the western United States and Canada: direct and indirect effects. BioScience 60, 602–613. https://doi.org/10.1525/bio.2010.60.8.6.

Biondi, F., Qeadan, F., 2008. A theory-driven approach to tree-ring standardization: defining the biological trend from expected basal area increment. Tree-Ring Research 64, 81–97.

Bjornstad, O.N., 2019. Ncf: Spatial Covariance Functions. https://doi.org/10.3959/2008-6.1.

Boone, C.K., Aukema, B.H., Bohlmann, J.r., Carroll, A.L., Raffa, K.F., 2011. Efficacy of tree defense physiology varies with bark beetle population density: a basis for positive feedback in eruptive species. Can. J. For. Res. 41, 1174–1188. https://doi.org/10.1139/x11-041.

Brunner, I., Herzog, C., Dawes, M.A., Arend, M., Sperisen, C., 2015. How tree roots respond to drought. Front. Plant Sci. 6, 547. https://doi.org/10.3389/fpls.2015.00547.

Bugmann, H., Seidl, R., Hartig, F., Bohn, F., Brůna, J., Cailleret, M., François, L., Heinke, J., Henrot, A.J., Hickler, T., 2019. Tree mortality submodels drive simulated long-term forest dynamics: assessing 15 models from the stand to global scale. Ecosphere 10, e02616. https://doi.org/10.1002/ecs2.2616.

Bunn, A.G., 2008. A dendrochronology program library in R (dplR). Dendrochronologia 26, 115–124. https://doi.org/10.1016/j.dendro.2008.01.002.

Cailleret, M., Jansen, S., Robert, E.M., Desoto, L., Aakala, T., Antos, J.A., Beikircher, B., Bigler, C., Bugmann, H., Caccianiga, M., 2017. A synthesis of radial growth patterns preceding tree mortality. Glob. Chang. Biol. 23, 1675–1690. https://doi.org/10.1111/gcb.13535.

Cailleret, M., Dakos, V., Jansen, S., Robert, E.M., Aakala, T., Amoroso, M.M., Antos, J.A., Bigler, C., Bugmann, H., Caccianiga, M., 2019. Early-warning signals of individual tree mortality based on annual radial growth. Front. Plant Sci. 9, 1964. https://doi.org/10.3389/fpls.2018.01964.

Camarero, J.J., Gazol, A., Sangüesa-Barreda, G., Oliva, J., Vicente-Serrano, S.M., 2015. To die or not to die: early warnings of tree dieback in response to a severe drought. J. Ecol. 103, 44–57. https://doi.org/10.1111/1365-2745.12295.

Cavin, L., Mountford, E.P., Peterken, G.F., Jump, A.S., 2013. Extreme drought alters competitive dominance within and between tree species in a mixed forest stand. Funct. Ecol. 27, 1424–1435. https://doi.org/10.1111/1365-2435.12126.

Cole, K.L., Fisher, J., Arundel, S.T., Cannella, J., Swift, S., 2008. Geographical and climatic limits of needle types of one-and two-needled pinyon pines. J. Biogeogr. 35, 257–269. https://doi.org/10.1111/j.1365-2699.2007.01786.x.

Cook, E.R., Kairiukstis, L.A. (Eds.), 2013. Methods of Dendrochronology: Applications in the Environmental Sciences. Springer Science & Business Media.

Cooper, L.A., Reed, C.C., Ballantyne, A.P., 2018. Mountain pine beetle attack faster growing lodgepole pine at low elevations in western Montana, USA. For. Ecol. Manag. 427, 200–207. https://doi.org/10.1016/j.foreco.2018.05.048.

Csank, A.Z., Miller, A.E., Sherriff, R.L., Berg, E.E., Welker, J.M., 2016. Tree-ring isotopes reveal drought sensitivity in trees killed by spruce beetle outbreaks in south-Central Alaska. Ecol. Appl. 26, 2001–2020. https://doi.org/10.1002/eap.1365.

Dale, V.H., Joyce, L.A., McNulty, S., Neilson, R.P., Ayres, M.P., Flannigan, M.D., Hanson, P.J., Irland, L.C., Lugo, A.E., Peterson, C.J., Simberloff, D., Swanson, F.J., Stocks, B.J., Michael Wotton, B., 2001. Climate change and forest disturbances: climate change can affect forests by altering the frequency, intensity, duration, and timing of fire, drought, introduced species, insect and pathogen outbreaks, hurricanes, windstorms, ice storms, or landslides. BioScience 51, 723–734. https://doi.org/10.1641/0006-3568(2001)051[0723:CCAFD]2.0.CO;2.

Diffenbaugh, N.S., Swain, D.L., Touma, D., 2015. Anthropogenic warming has increased drought risk in California. Proc. Natl. Acad. Sci. 112, 3931–3936. https://doi.org/10.1073/pnas.1422385112.

Dobbertin, M., 2005. Tree growth as indicator of tree vitality and of tree reaction to environmental stress: a review. Eur. J. For. Res. 124, 319–333. https://doi.org/10.1007/s10342-005-0085-3.

Duffy, J.E., McCarroll, D., Barnes, A., Ramsey, C.B., Davies, D., Loader, N.J., Miles, D., Young, G.H., 2017. Short-lived juvenile effects observed in stable carbon and oxygen isotopes of UK oak trees and historic building timbers. Chem. Geol. 472, 1–7. https://doi.org/10.1016/j.chemgeo.2017.09.007.

Egan, J.M., Jacobi, W.R., Negron, J.F., Smith, S.L., Cluck, D.R., 2010. Forest thinning and subsequent bark beetle-caused mortality in Northeastern California. For. Ecol. Manag. 260, 1832–1842. https://doi.org/10.1016/j.foreco.2010.08.030.

Egan, J.M., Sloughter, J.M., Cardoso, T., Trainor, P., Wu, K., Safford, H., Fournier, D., 2016. Multi-temporal ecological analysis of Jeffrey pine beetle outbreak dynamics within the Lake Tahoe Basin. Popul. Ecol. 58, 441–462. https://doi.org/10.1007/s10144-016-0545-2.

Farquhar, G., Richards, R., 1984. Isotopic composition of plant carbon correlates with water-use efficiency of wheat genotypes. Funct. Plant Biol. 11, 539–552. https://doi.org/10.1071/PP9840539.

Farquhar, G.D., O'Leary, M.H., Berry, J.A., 1982. On the relationship between carbon isotope discrimination and the intercellular carbon dioxide concentration in leaves. Funct. Plant Biol. 9, 121–137. https://doi.org/10.1071/PP9820121.

Farquhar, G.D., Ehleringer, J.R., Hubick, K.T., 1989. Carbon isotope discrimination and photosynthesis. Annu. Rev. Plant Biol. 40, 503–537. https://doi.org/10.1146/annurev.pp.40.060189.002443.

Ferrell, G., W. Otrosina, and C. Demars Jr. 1994. Predicting susceptibility of white fir during a drought-associated outbreak of the fir engraver, Scolytus ventralis, in California. Can. J. For. Res. 24:302–305. doi:https://doi.org/10.1139/x94-043.

Ferrenberg, S., Kane, J., Mitton, J., 2014. Resin duct characteristics associated with tree resistance to bark beetles across lodgepole and limber pines. Oecologia 174, 1283–1292. https://doi.org/10.1007/s00442-013-2841-2.

Fettig, C.J., Klepzig, K.D., Billings, R.F., Munson, A.S., Nebeker, T.E., Negrón, J.F., Nowak, J.T., 2007. The effectiveness of vegetation management practices for prevention and control of bark beetle infestations in coniferous forests of the western and southern United States. For. Ecol. Manag. 238, 24–53. https://doi.org/10.1016/j.foreco.2006.10.011.

Fettig, C.J., Mortenson, L.A., Bulaon, B.M., Foulk, P.B., 2019. Tree mortality following drought in the central and southern Sierra Nevada, California, US. For. Ecol. Manag. 432, 164–178. https://doi.org/10.1016/j.foreco.2018.09.006.

Gärtner, H., Nievergelt, D., 2010. The core-microtome: a new tool for surface preparation on cores and time series analysis of varying cell parameters. Dendrochronologia 28, 85–92. https://doi.org/10.1016/j.dendro.2009.09.002.

Gaylord, M.L., Kolb, T.E., Pockman, W.T., Plaut, J.A., Yepez, E.A., Macalady, A.K., Pangle, R.E., McDowell, N.G., 2013. Drought predisposes piñon–juniper woodlands to insect attacks and mortality. New Phytol. 198, 567–578. https://doi.org/10.1111/nph.12174.

Gaylord, M.L., Kolb, T.E., McDowell, N.G., 2015. Mechanisms of piñon pine mortality after severe drought: a retrospective study of mature trees. Tree Physiol. https://doi.org/10.1093/treephys/tpv038.

Gessler, A.M., Ferrio, J.P., Hommel, R., Treydte, K., Werner, R.A., Monson, R.K., 2014. Stable isotopes in tree rings: towards a mechanistic understanding of isotope fractionation and mixing processes from the leaves to the wood. Tree Physiol. 34, 796–818. https://doi.org/10.1093/treephys/tpu040.

Gessler, A.M., Cailleret, J. Joseph, Schönbeck, L., Schaub, M., Lehmann, M., Treydte, K., Rigling, A., Timofeeva, G., Saurer, M., 2018. Drought induced tree mortality–a tree-ring isotope based conceptual model to assess mechanisms and predispositions. New Phytol. 219, 485–490. https://doi.org/10.1111/nph.15154.

Goulden, M., Bales, R., 2019. California forest die-off linked to multi-year deep soil drying in 2012–2015 drought. Nat. Geosci. 12, 632–637. https://doi.org/10.1038/s41561-019-0388-5.

Harlow, B., Marshall, J., Robinson, A., 2006. A multi-species comparison of δ13C from whole wood, extractive-free wood and holocellulose. Tree Physiol. 26, 767–774. https://doi.org/10.1093/treephys/26.6.767.

Hartmann, H., Moura, C.F., Anderegg, W.R., Ruehr, N.K., Salmon, Y., Allen, C.D., Arndt, S.K., Breshears, D.D., Davi, H., Galbraith, D., 2018. Research frontiers for improving our understanding of drought-induced tree and forest mortality. New Phytol. 218, 15–28. https://doi.org/10.1111/nph.15048.

Hereş, A.-M., Martínez-Vilalta, J., López, B.C., 2012. Growth patterns in relation to drought-induced mortality at two Scots pine (Pinus sylvestris L.) sites in NE Iberian Peninsula. Trees 26, 621–630. https://doi.org/10.1007/s00468-011-0628-9.

Hereş, A.-M., Voltas, J., López, B.C., Martínez-Vilalta, J., 2014. Drought-induced mortality selectively affects scots pine trees that show limited intrinsic water-use efficiency responsiveness to raising atmospheric CO2. Funct. Plant Biol. 41, 244–256. https://doi.org/10.1071/FP13067.

Holmes, R.L., 1983. Computer-Assisted Quality Control in Tree-Ring Dating and Measurement.

Hood, S.M., Reed, C.C., Kane, J.M. In Review. Axial resin duct quantification in tree rings: a functional defense trait. MethodsX. Submitted for publication.

Hood, S., Sala, A., 2015. Ponderosa pine resin defenses and growth: metrics matter. Tree Physiol. 35, 1223–1235. https://doi.org/10.1093/treephys/tpv098.

Hood, S., Sala, A., Heyerdahl, E.K., Boutin, M., 2015. Low-severity fire increases tree defense against bark beetle attacks. Ecology 96, 1846–1855. https://doi.org/10.1890/14-0487.1.

Hood, S.M., Baker, S., Sala, A., 2016. Fortifying the forest: thinning and burning increase resistance to a bark beetle outbreak and promote forest resilience. Ecol. Appl. 26, 1984–2000. https://doi.org/10.1002/eap.1363.

Huang, J., Kautz, M., Trowbridge, A.M., Hammerbacher, A., Raffa, K.F., Adams, H.D., Goodsman, D.W., Xu, C, Meddens, A.J., Kandasamy, D., Gershenzon, J., 2020. Tree defence and bark beetles in a drying world: carbon partitioning, functioning and modelling. New Phytol. 225, 26–36. https://doi.org/10.1111/nph.16173.

IPCC, 2014. In: Core Writing Team, Pachauri, R.K., Meyer, L.A. (Eds.), Climate Change 2014: Synthesis Report. Contribution of Working Groups I, II and III to the Fifth Assessment Report of the Intergovernmental Panel on Climate Change. IPCC, Geneva, Switzerland (151 pp).

Kane, J.M., Kolb, T.E., 2010. Importance of resin ducts in reducing ponderosa pine mortality from bark beetle attack. Oecologia 164, 601–609. https://doi.org/10.1007/s00442-010-1683-4.

Kichas, N.E., Hood, S.M., Pederson, G.T., Everett, R.G., McWethy, D.B., 2020. Whitebark pine (Pinus albicaulis) growth and defense in response to mountain pine beetle outbreaks. For. Ecol. Manag. 457, 117736. https://doi.org/10.1016/j.foreco.2019.117736.

Kolb, T.E., Fettig, C.J., Ayres, M.P., Bentz, B.J., Hicke, J.A., Mathiasen, R., Stewart, J.E., Weed, A.S., 2016. Observed and anticipated impacts of drought on forest insects and diseases in the United States. For. Ecol. Manag. 380, 321–334. https://doi.org/10.1016/j.foreco.2016.04.051.

Kolb, T., Keefover-Ring, K., Burr, S.J., Hofstetter, R., Gaylord, M., Raffa, K.F., 2019. Drought-mediated changes in tree physiological processes weaken tree defenses to bark beetle attack. J. Chem. Ecol. 45, 888–900. https://doi.org/10.1007/s10886-019-01105-0.

Leavitt, S.W., 2010. Tree-ring C–H–O isotope variability and sampling. Sci. Total Environ. 408, 5244–5253. https://doi.org/10.1016/j.scitotenv.2010.07.057.

Leavitt, S.W., Danzer, S.R., 1993. Method for batch processing small wood samples to holocellulose for stable-carbon isotope analysis. Anal. Chem. 65, 87–89. https://doi.org/10.1021/ac00049a017.

Lebourgeois, F., Eberle, P., Mérian, P., Seynave, I., 2014. Social status-mediated tree-ring responses to climate of Abies alba and Fagus sylvatica shift in importance with increasing stand basal area. For. Ecol. Manag. 328, 209–218. https://doi.org/10.1016/j.foreco.2014.05.038.

Lehmann, M.M., Saurer, M., Fonti, M.V., Siegwolf, R.T., Bigler, C., 2018. Compound-specific carbon isotopes and concentrations of carbohydrates and organic acids as indicators of tree decline in mountain pine. Forests 9, 363. https://doi.org/10.3390/f9060363.

Liu, Y., Kumar, M., Katul, G.G., Porporato, A., 2019. Reduced resilience as an early warning signal of forest mortality. Nat. Clim. Chang. 9, 880–885. https://doi.org/10.1038/s41558-019-0583-9.

Lloret, F., Peñuelas, J., Prieto, P., Llorens, L., Estiarte, M., 2009. Plant community changes induced by experimental climate change: seedling and adult species composition. Perspectives in Plant Ecology, Evolution and Systematics 11, 53–63. https://doi.org/10.1016/j.ppees.2008.09.001.

Macalady, A.K., Bugmann, H., 2014. Growth-mortality relationships in Piñon pine (Pinus edulis) during severe droughts of the past century: shifting processes in space and time. PLoS One 9, e92770. https://doi.org/10.1371/journal.pone.0092770.

Martín-Benito, D., Cherubini, P., Del Río, M., Cañellas, I., 2008. Growth response to climate and drought in Pinus nigra Arn. Trees of different crown classes. Trees 22, 363–373. https://doi.org/10.1007/s00468-007-0191-6.

Martínez-Vilalta, J., Lloret, F., 2016. Drought-induced vegetation shifts in terrestrial ecosystems: the key role of regeneration dynamics. Glob. Planet. Chang. 144, 94–108. https://doi.org/10.1016/j.gloplacha.2016.07.009.

Martínez-Vilalta, J., Sala, A., Asensio, D., Galiano, L., Hoch, G., Palacio, S., Piper, F.I., Lloret, F., 2016. Dynamics of non-structural carbohydrates in terrestrial plants: a global synthesis. Ecol. Monogr. 86, 495–516. https://doi.org/10.1002/ecm.1231.

de la Mata, R., Hood, S., Sala, A., 2017. Insect outbreak shifts the direction of selection from fast to slow growth rates in the long-lived conifer Pinus ponderosa. Proc. Natl. Acad. Sci. 114, 7391–7396. https://doi.org/10.1073/pnas.1700032114.

McCarroll, D., Loader, N.J., 2004. Stable isotopes in tree rings. Quat. Sci. Rev. 23, 771–801. https://doi.org/10.1016/j.quascirev.2003.06.017.

McDowell, N., Pockman, W.T., Allen, C.D., Breshears, D.D., Cobb, N., Kolb, T., Plaut, J., Sperry, J., West, A., Williams, D.G., Yepez, E.A., 2008. Mechanisms of plant survival and mortality during drought: why do some plants survive while others succumb to drought? New Phytol. 178, 719–739. https://doi.org/10.1111/j.1469-8137.2008.02436.x.

McDowell, N.G., Allen, C.D., Marshall, L., 2010. Growth, carbon-isotope discrimination, and drought-associated mortality across a Pinus ponderosa elevational transect. Glob. Chang. Biol. 16, 399–415. https://doi.org/10.1111/j.1365-2486.2009.01994.x.

Meddens, A.J., Hicke, J.A., Macalady, A.K., Buotte, P.C., Cowles, T.R., Allen, C.D., 2015. Patterns and causes of observed piñon pine mortality in the southwestern United States. New Phytol. 206, 91–97. https://doi.org/10.1111/nph.13193.

Mohan, J.E., Cowden, C.C., Baas, P., Dawadi, A., Frankson, P.T., Helmick, K., Hughes, E., Khan, S., Lang, A., Machmuller, M., 2014. Mycorrhizal fungi mediation of terrestrial ecosystem responses to global change: mini-review. Fungal Ecol. 10, 3–19. https://doi.org/10.1016/j.funeco.2014.01.005.

Natural Resources Conservation Service (NRCS), United States Department of Agriculture, 2019. Web soil survey. Available online at: https://websoilsurvey.nrcs.usda.gov/.

Negrón, J.F., Wilson, J.L., 2003. Attributes associated with probability of infestation by the piñon ips, Ips confusus (Coleoptera: Scolytidae), in piñon pine, Pinus edulis. Western North American Naturalist 63, 4.

Paz-Kagan, T., Brodrick, P.G., Vaughn, N.R., Das, A.J., Stephenson, N.L., Nydick, K.R., Asner, G.P., 2017. What mediates tree mortality during drought in the southern Sierra Nevada? Ecol. Appl. 27, 2443–2457. https://doi.org/10.1002/eap.1620.

Phillips, R.P., Ibáñez, I., D'Orangeville, L., Hanson, P.J., Ryan, M.G., McDowell, N.G., 2016. A belowground perspective on the drought sensitivity of forests: towards improved understanding and simulation. For. Ecol. Manag. 380, 309–320. https://doi.org/10.1016/j.foreco.2016.08.043.

Pile, L.S., Meyer, M.D., Rojas, R., Roe, O., Smith, M.T., 2019. Drought impacts and compounding mortality on forest trees in the southern Sierra Nevada. Forests 10, 237. https://doi.org/10.3390/f10030237.

R Core Team, 2019. R: A Language and Environment for Statistical Computing. R Foundation for Statistical Computing, Vienna, Austria.

Raffa, K.M., 2014. Terpenes tell different tales at different scales: glimpses into the chemical ecology of conifer - bark beetle - microbial interactions. J. Chem. Ecol. 40, 1–20. https://doi.org/10.1007/s10886-013-0368-y.

Raffa, K.F., Aukema, B.H., Bentz, B.J., Carroll, A.L., Hicke, J.A., Turner, M.G., Romme, W.H., 2008. Cross-scale drivers of natural disturbances prone to anthropogenic amplification: the dynamics of bark beetle eruption. BioScience 58, 501–517. https://doi.org/10.1641/B580607.

Restaino, C., Young, D.J., Estes, B., Gross, S., Wuenschel, A., Meyer, M., Safford, H., 2019. Forest structure and climate mediate drought-induced tree mortality in forests of the Sierra Nevada, USA. Ecol. Appl. 29, e01902. https://doi.org/10.1002/eap.1902.

Rizopoulos, D., 2019. GLMMadaptive: Generalized Linear Mixed Models Using Adaptive Gaussian Quadrature.

Sapes, G., Roskilly, B., Dobrowski, S., Maneta, M., Anderegg, W.R., Martinez-Vilalta, J., Sala, A., 2019. Plant water content integrates hydraulics and carbon depletion to predict drought-induced seedling mortality. Tree Physiol. 39, 1300–1312. https://doi.org/10.1093/treephys/tpz062.

Schweingruber, F.H., 1996. Tree Rings and Environment: Dendroecology. Paul Haupt AG Bern.

Sevanto, S., McDowell, N.G., Dickman, L.T., Pangle, R., Pockman, W.T., 2014. How do trees die? A test of the hydraulic failure and carbon starvation hypotheses. Plant Cell Environ. 37, 153–161. https://doi.org/10.1111/pce.12141.

Stephenson, N.L., Das, A.J., Ampersee, N.J., Bulaon, B.M., Yee, J.L., 2019. Which trees die during drought? The key role of insect host-tree selection. J. Ecol. https://doi.org/10.1111/1365-2745.13176.

Sthultz, C.M., Gehring, C.A., Whitham, T.G., 2009. Deadly combination of genes and drought: increased mortality of herbivore-resistant trees in a foundation species. Glob. Chang. Biol. 15, 1949–1961. https://doi.org/10.1111/j.1365-2486.2009.01901.x.

Stokes, M.A., Smiley, L., 1968. An Introduction to Tree-Ring Dating. University of Chicago Press, Chicago, Illinois.

Suarez, M.L., Ghermandi, L., Kitzberger, T., 2004. Factors predisposing episodic drought-induced tree mortality in Nothofagus–site, climatic sensitivity and growth trends. J. Ecol. 92, 954–966. https://doi.org/10.1111/j.1365-2745.2004.00941.x.

Trenberth, K.E., Dai, A., Van Der Schrier, G., Jones, P.D., Barichivich, J., Briffa, K.R., Sheffield, J., 2014. Global warming and changes in drought. Nat. Clim. Chang. 4, 17. https://doi.org/10.1038/nclimate2067.

USDA Forest Service, 2019. Survey Finds 18 Million Trees Died in California in 2018.

Voltas, J., Camarero, J.J., Carulla, D., Aguilera, M., Ortiz, A., FERRIO, J.P., 2013. A retrospective, dual-isotope approach reveals individual predispositions to winter-drought induced tree dieback in the southernmost distribution limit of scots pine. Plant Cell Environ. 36, 1435–1448. https://doi.org/10.1111/pce.12072.

Warren, C.R., McGrath, J.F., Adams, M.A., 2001. Water availability and carbon isotope discrimination in conifers. Oecologia 127, 476–486. https://doi.org/10.1007/s004420000609.

White, J.W.C., Vaughn, B.H., Michel, S.E., 2015. University of Colorado, Institute of Arctic and Alpine Research (INSTAAR), Stable Isotopic Composition of Atmospheric Carbon Dioxide (13C and 18O) from the NOAA ESRL Carbon Cycle Cooperative Global Air Sampling Network, 1990–2014, Version: 2015-10-26.

Wood, D.L., 1982. The Bark and Ambrosia Beetles of North and Central America (Coleoptera: Scolytidae), a Taxonomic Monograph. Great Basin Naturalist Memoirs, No. 6. Brigham Young University, Provo, UT.

Zadworny, M., Jagodziński, A.M., Łakomy, P., Mucha, J., Oleksyn, J., Rodríguez-Calcerrada, J., Ufnalski, K., 2019. Regeneration origin affects radial growth patterns preceding oak decline and death – insights from tree-ring δ13C and δ18O. Agric. For. Meteorol. 278, 107685. https://doi.org/10.1016/j.agrformet.2019.107685.

Zang, C., Biondi, F., 2015. Treeclim: an R package for the numerical calibration of proxy-climate relationships. Ecography 38, 431–436. https://doi.org/10.1111/ecog.01335.

Zhao, S., Erbilgin, N., 2019. Larger resin ducts are linked to the survival of lodgepole pine trees during mountain pine beetle outbreak. Front. Plant Sci. 10, 1459. https://doi.org/10.3389/fpls.2019.01459.

Zhao, M., Running, S.W., 2010. Drought-induced reduction in global terrestrial net primary production from 2000 through 2009. Science 329, 940–943. https://doi.org/10.1126/science.1192666.